2007

REPAIR AND EFFECTS OF THE 8-OXOG LESION IN DNA

James Joseph Covino
The University of Montana

REPAIR AND EFFECTS OF THE 8-OXOG LESION IN DNA

by

James Joseph Covino II

B.S. Chemistry, The University of Mary Washington, 2003

Thesis
Presented in partial fulfillment of the requirements
for the degree of

Masters of Science
in Chemistry

The University of Montana
Missoula, MT

Autumn 2007

Approved by:

Dr. David A. Strobel, Dean
Graduate School

Kent D. Sugden, Chair
Department of Chemistry

Brooke Martin
Department of Chemistry

Holly Thompson
Department of Chemistry

Nigel Priestly
Department of Chemistry

Fernando Cardozo
Center for Environmental Health Sciences

Covino, James J., M.S. November 2007 Chemistry

Repair and Effects of the 8-oxoG Lesion in DNA

Chairperson: Kent D. Sugden

Eukaryotic DNA is packaged in a condensed state with histone proteins. The minimal structural unit within packaged eukaryotic DNA is the nucleosome core particle (NCP). The NCP consists of a 146 bp DNA fragment wrapped around an octamer of histone core proteins. Nucleosome core particle formation induces DNA structural changes and reduced DNA accessibility providing a very different setting than that commonly modeled by *in vitro* studies. *In vitro* reconstituted NCP provide a controlled environment that more closely models eukaryotic DNA than studies using naked DNA. Reconstituted NCP studies of DNA damage have exhibited a spectrum of effects compared to naked DNA ranging from protective, enhanced, and no effect. The nature of the effect appears to be related to the type of oxidant, its sterics and interactions with the histone surface and altered DNA structure. While there is differences in efficiencies of oxidation of nucleobases throughout the nucleosome, nucleobase oxidation is still widespread within the genome.

DNA repair processes that combat global DNA oxidation are crucial to cell survival. One major cellular repair mechanism that is employed to remove DNA damage is base excision repair (BER). The BER pathway involves the concerted activity of a small number of proteins which catalyze individual reactions in a chemical pathway that repairs single nucleotide lesions. *In vivo*, the majority of DNA is wrapped around histones and the repair machinery of BER has to work within or around the structure of the nucleosome and deal with a distorted DNA structure and reduced accessibility due to the presence of bulky histone proteins.

To address the questions of DNA damage and repair in the nucleosome an *in-vitro* nucleosomal system was established by reconstituting purified histones and a 154 bp wrapping fragment from the *Xenopus borealis* 5S rRNA gene to form individual nucleosome core particles (NCP). The effect of nucleosome formation on chromium-mediated DNA damage and the efficiency of BER glycosylase cleavage of the lesion 8-oxoG were investigated.

Base excision of 8-oxoG by Fpg and hOGG1 indicated that: i) the position of the lesion 8-oxoG in naked DNA can influence BER activity; ii) nucleosomal formation decreases the activity of these BER enzymes by as much as 2.5 fold with a rotational dependence exhibiting increased cleavage towards the more accessible lesion; iii) the rotational dependence for both Fpg and hOGG1 was almost identical, however hOGG1 showed better cleavage in the nucleosome setting relative to free DNA at earlier time points.

An additional study was done to examine the potential of 8-oxoG lesions to mimic cytosine methylation effects with regard to the activity of a methyl-sensitive endonuclease. Using enzyme cleavage assays the effects of placing an 8-oxoG or methylated cytosine into the recognition sequence of a restriction endonuclease, *Not*I, were investigated. Results indicate identical inhibitory effects between 8-oxoG and cytosine methylation, hinting at a potential role of 8-oxoG in epigenetics.

Acknowledgments

Dedicated to the science teachers who inspired and challenged me

Dr. Horace Puglisi
Dr. John Maddalena
Adam Weiss
Dr. Leanna Giancarlo
Dr. Brooke Martin and Dr. Kent Sugden

"The teacher who walks in the shadow of the temple, among his followers, gives not of his wisdom but rather of his faith and his lovingness.

If he is indeed wise he does not bid you enter the house of wisdom, but rather leads you to the threshold of your own mind.

The astronomer may speak to you of his understanding of space, but he cannot give you his understanding.

The musician may sing to you of the rhythm which is in all space, but he cannot give you the ear which arrests the rhythm nor the voice that echoes it.

And he who is versed in the science of numbers can tell of the regions of weight and measure, but he cannot conduct you thither.

For the vision of one man lends not its wings to another man." (Kahlil Gibran, The Prophet)

Table of Contents

List of Abbreviations

8-oxoG:	8-oxo-7,8-dihydro-2'-deoxyguanosine
APE1	Human apurinic/apyrimidinic (AP) endonuclease, also known as HAP 1 or Ref-1
BER:	base excision repair
BCA:	bicinchoninic acid
DNA:	deoxyribonucleic acid
EDTA:	ethylenediaminetetraacetic acid
Ehba:	2-ethyl-2-hydroxybutyrate
EMSA:	electrophoretic mobility shift assay, gel shift assay
Fpg:	formamidopyrimidine BER glycosylase
Gh:	guanidinohydantoin
G (dG):	guanine
hOGG1	human 8-oxoguanine BER glycosylase 1
HPLC:	high performance liquid chromatography
NCP:	nucleosome core particle
NEB:	New England Biolabs
NER:	nucleotide excision repair
PAGE:	polyacrylamide gel electrophoresis
PCR:	polymerase chain reaction
Salen:	*N*,*N*',-bis(salicylidene) ethylenediamine
SDS:	sodium dodecyl sulfate
Sp:	spiroiminodihydantoin

List of Figures

Chapter 1: Nucleosomal DNA Damage

1.1 Introduction: The Nucleosome

The human genome of 3 billion base pairs would extend over a meter if unraveled, however nature has engineered a way to compact it into a nucleus with a diameter of only 10^{-5} meters [1]. Such compaction is possible due to histone proteins that mediate the folding of DNA into nucleosomes, and subsequently allow the formation of higher order chromatin structures that facilitate the compaction of DNA up to 10,000 fold its naked length [2]. The foundation of this engineering feat is the nucleosome. The nucleosome consists of an octamer of core histones - two dimers of H2A-H2B and a tetramer of H3-H4 , 146 base pairs of wrapped DNA in a left handed superhelix, and a linker histone, such as H1 or H5.

DNA - histone binding occurs through a vast number of hydrogen bonds and the coulombic interactions between positively charged amino acids on the histone surface and the abundance of negatively charged phosphate oxygens in the DNA backbone [3,4]. The majority of these bonds are between arginine or lysine and the DNA backbone [3,4]. Hydrogen bonding to the phosphate backbone can also occur through histidine as well as the amino terminal end of amino acid chains [3,4].

Nucleosomal formation reduces accessibility to DNA in addition to producing DNA deformation, figure 1.1. Overall nucleosomal DNA is stretched leaving a periodicity average of 10.2 base pairs per turn compared with 10.4 base pairs per turn in naked B form DNA [1,3]. Such DNA deformation is non-uniform with areas of increased bending and altered periodicity. Early studies utilizing highly reactive singlet oxygen and hydroxyl radical cleavage illustrated a non-uniform deformed state in the

nucleosome. Singlet oxygen preferentially reacted towards DNA 1.5 turns on either side of the center of the nucleosome, which is referred to as the dyad [5]. Hydroxyl radical cleavage illustrated an altered helical periodicity with the three turns of DNA over the dyad having 10.7 bp/turn and the remaining turns of DNA having 10.0 bp/turn [1]. The 2.8 Å resolution crystal structure of the nucleosome confirmed the non-uniform deformed state revealing a maximum curvature and radius at 1.5 and 4.5 turns on either side of the dyad [4].

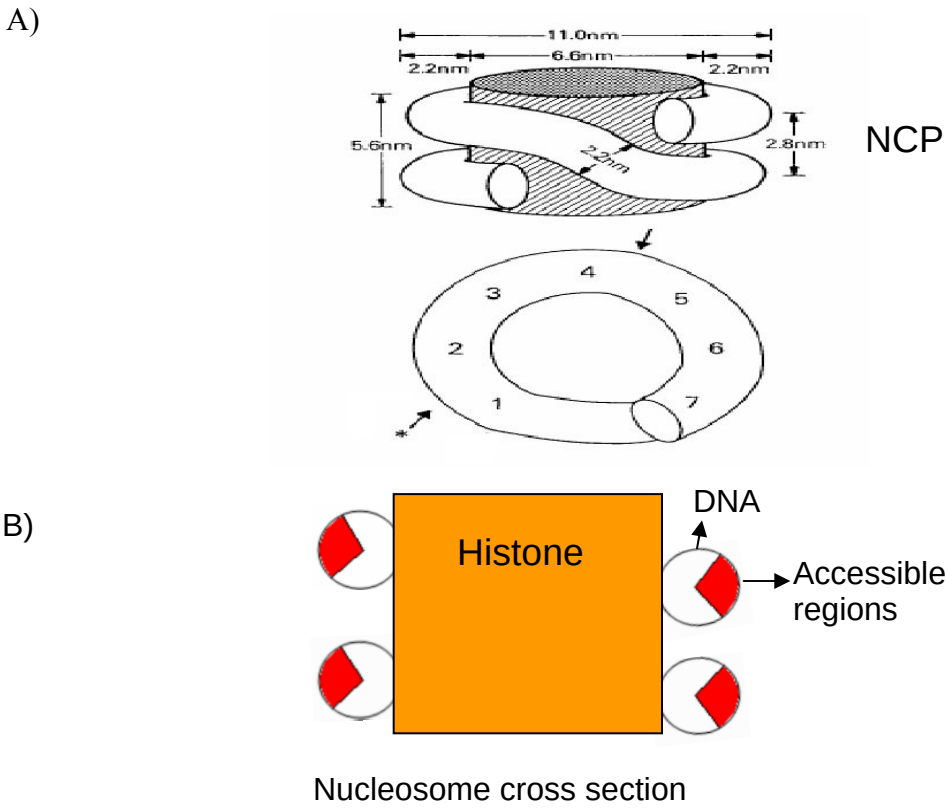

Figure 1.1 Illustration of DNA wrapping of DNA around the histone octamer core. A) Top: Dimensions of the nucleosome: histone octamer represented by a cylinder, DNA by a tube. Bottom: Path of one turn of nucleosomal DNA: the numbers represent one turn of DNA, and arrows represent places of increased distortion. B) Nucleosome cross section showing rotational accessibility of DNA. Orange square represents histone, circles represent DNA. Red regions indicate solution accessible grooves in nucleosomal DNA [1].

Nucleosomal DNA exhibits a sequence dependence to nucleosome formation. Sequence dependent wrapping efficiencies have been correlated to the ease of compression of the minor grooves facing the histone protein, which facilitates the bending of the superhelix around the histone octamer. A-T base pairs are more easily compressed into the minor groove facing the histone surface compared with G-C sequences. DNA and histones will position themselves to maximize such interactions [1-3]. Research has illustrated a high degree of variation in DNA sequence affinities for nucleosome formation with a 1000 fold difference between the lowest and highest affinity DNA [6].

1.2 Chromium induced DNA damage

The cellular uptake and metabolism of chromate is described by the classical uptake-reduction model [7]. Hexavalent chromium, being structurally similar with phosphate and sulfate, allows for passive uptake through nonselective anionic membrane channels, figure 1.2. Once internalized, chromate is rapidly reduced to Cr(III) by endogenous reductants resulting in the unidirectional accumulation of chromium in the cell. Accumulations of intracellular chromium at concentrations greater than 1 mM have been observed in cell culture following a 10 μM chromate exposure in the extra-cellular media [8].

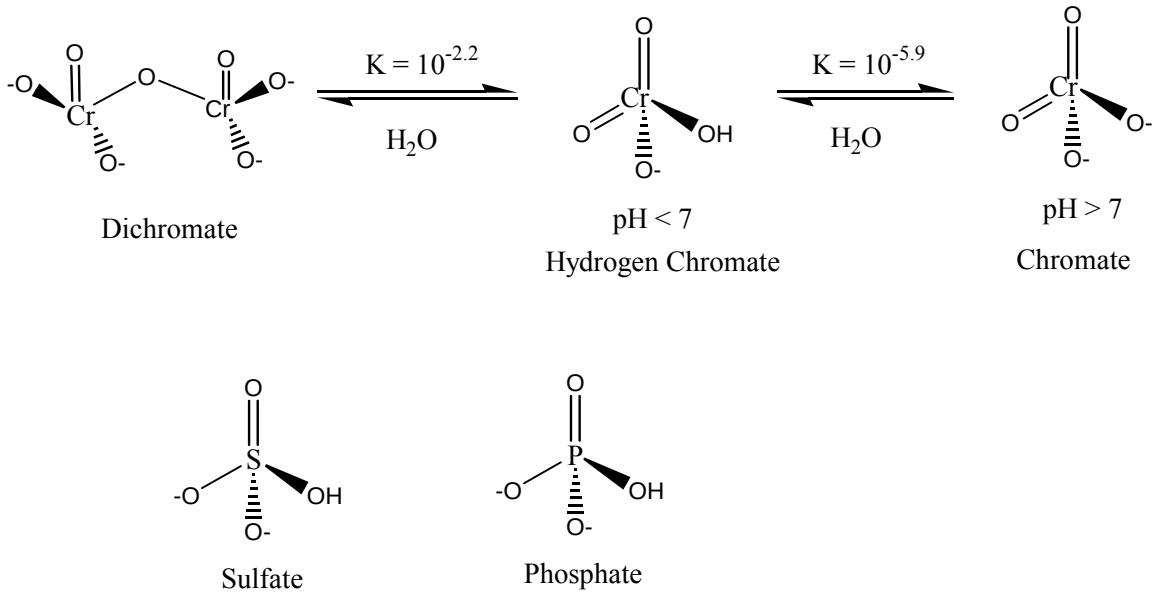

Figure 1.2 Chromate's structural similarity to sulfate and phosphate.

During the reduction of chromate a number of redox active species including reactive oxygen species (ROS), carbon- and sulfur-centered radicals and high valent chromium intermediate species, Cr(V) and Cr(IV) can be formed [10-24]. Nearly all of these species are capable of damaging DNA and yields of the different radical and metal species have been found to be dependent upon the type of reductant, the reductant/chromate ratio, pH, and oxygen concentration [10-24]. This wide assortment of potential DNA damaging agents has led to considerable discussion on the ultimate species responsible for DNA damage associated with chromate toxicity. Two different pathways have been proposed to account for DNA damage associated with chromate: the radical-mediated and the metal-mediated pathway (for a comprehensive explanation of these chromium mediated pathways see a recent review by Covino and Sugden, [9]).

Oxidative DNA damage as a result of Cr(VI) metabolism is believed to be one of the critical steps in the carcinogenetic effects of chromium. DNA oxidation can occur either at the deoxyribose sugar or at one of the four nucleic acid bases. Depending upon the site of oxidation, different lesions with differing mutagenic and toxic endpoints can be formed. Exposure to chromate has been shown to cause frank DNA strand breaks and abasic sites in bacterial and mammalian systems [25-31]. Frank strand breaks occur by oxidation of the deoxyribose sugar through electron abstraction. Thermodynamically, hydrogen atom abstraction is favored at the tertiary hydrogens, 1', 3', 4', over the secondary hydrogens, 2', 5', due to the enhanced stability of the resulting tertiary radicals over secondary radicals, figure 1.3. However, accessibility to the deoxyribose hydrogens in duplex DNA is a more controlling factor than thermodynamics alone. The increased solvent accessibility of the, 4' and 5' hydrogen(s) in duplex DNA makes them more likely to be abstracted than the thermodynamically favored but less accessible hydrogens [32].

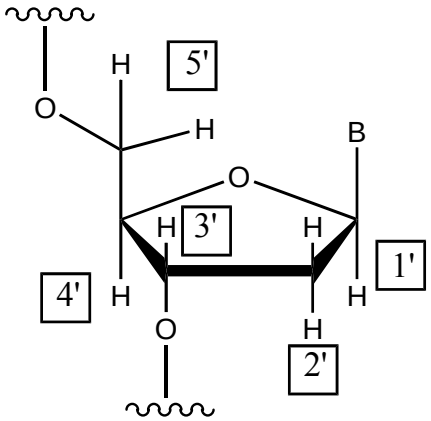

Radical Stability

1', 4', 3' > 2', 5'

Figure 1.3 Deoxyribose structure showing hydrogen atoms available for abstraction [9].

In addition to frank strand breaks exposure to chromate has been shown to cause nucleobase oxidation. Historically the 8-oxo-7,8-dihydro-2'-deoxyguanosine (8-oxoG) lesion has been associated with DNA nucleobase oxidation. 8-oxoG has been shown to form from a variety of redox active xenobiotics and endogenous metabolic processes. It has been estimated that 8-oxoG occurs at a frequency of ~10,000 bp per cell per day [33]. Because of its high frequency of occurrence, 8-oxoG has been implicated in the etiology of a large number of diseases and has been extensively used as a sensitive biomarker for oxidative damage to the cell [34-36]. The basis for the relatively high levels of cellular 8-oxoG formation is the enhanced sensitivity of the nucleobase guanine towards oxidation with respect to the other nucleic acid bases, figure 1.4 [37]. The sensitivity of guanine towards oxidation is further enhanced within duplex DNA in consecutive runs of guanines at the 5' of GG and GGG sequences [38]. In addition, the 8-oxoG lesion has a significantly lower reduction potential than the parent guanine, making it highly reactive toward further oxidation [39]. High valent chromium species have reduction potentials adequate to oxidize guanine within duplex DNA as well as the 8-oxoG lesion as the free nucleoside [40]. This thermodynamic basis explains chromate's propensity to cause exclusive guanine nucleobase damage forming both 8-oxoG as well as further oxidized guanine lesions.

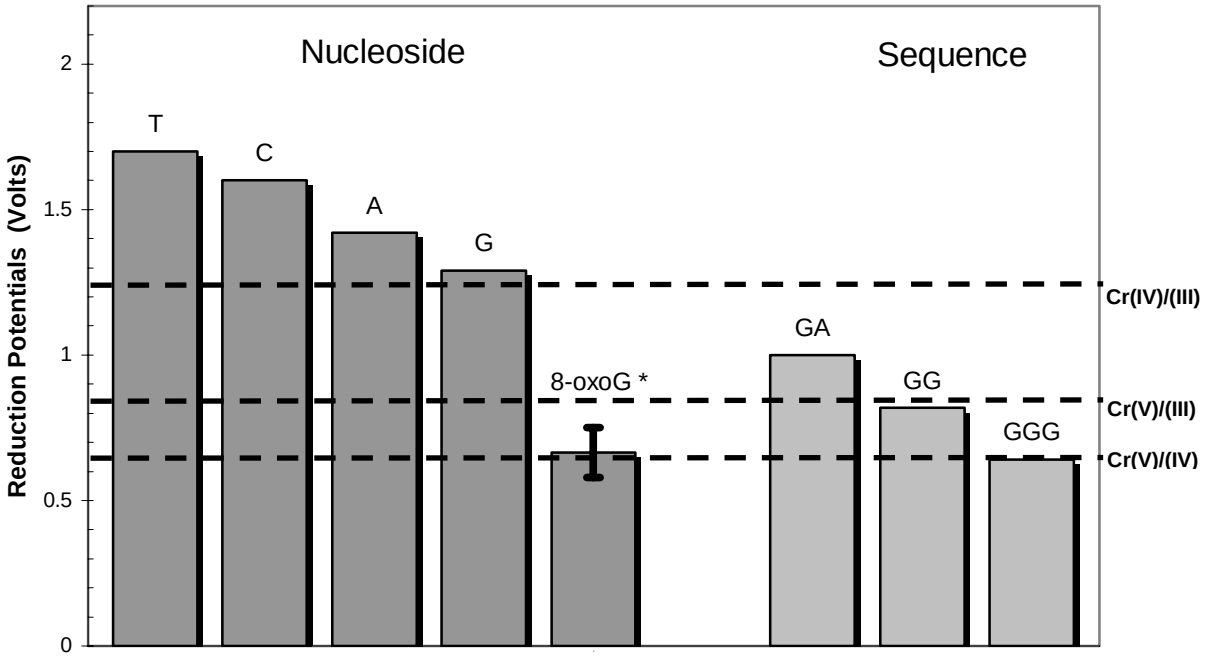

Figure 1.4 Reduction potentials of the four nucleobases, 8-oxoG, and guanine residues in DNA with consecutive runs. Dashed lines show the calculated reduction potentials of different high valent oxidation states of chromium with respect to the nucleoside or DNA [9].

The formation of 8-oxoG in DNA following chromate exposure has been shown in a variety of *in vitro*, cellular (*ex vivo*) and *in viv*o systems. However, not all chromate treated systems have shown 8-oxoG formation. Irrespective of these inconsistencies, the mechanism associated with 8-oxoG formation by chromate has historically been tied to reactive oxygen species (ROS) production, pathways a and c in figure 1.5. Recently a number of other mechanisms have been postulated to account for the formation of this ubiquitous guanine lesion. Two such mechanisms are the electron abstraction mechanism, pathway b in figure 1.5, and a metal-mediated oxo-atom transfer mechanism such as that shown in pathway d of figure 1.5. Regardless of the mechanism, the final 8-

oxoG product is the same for all pathways and discerning between these pathways to identify the ultimate species responsible for guanine oxidation is often difficult.

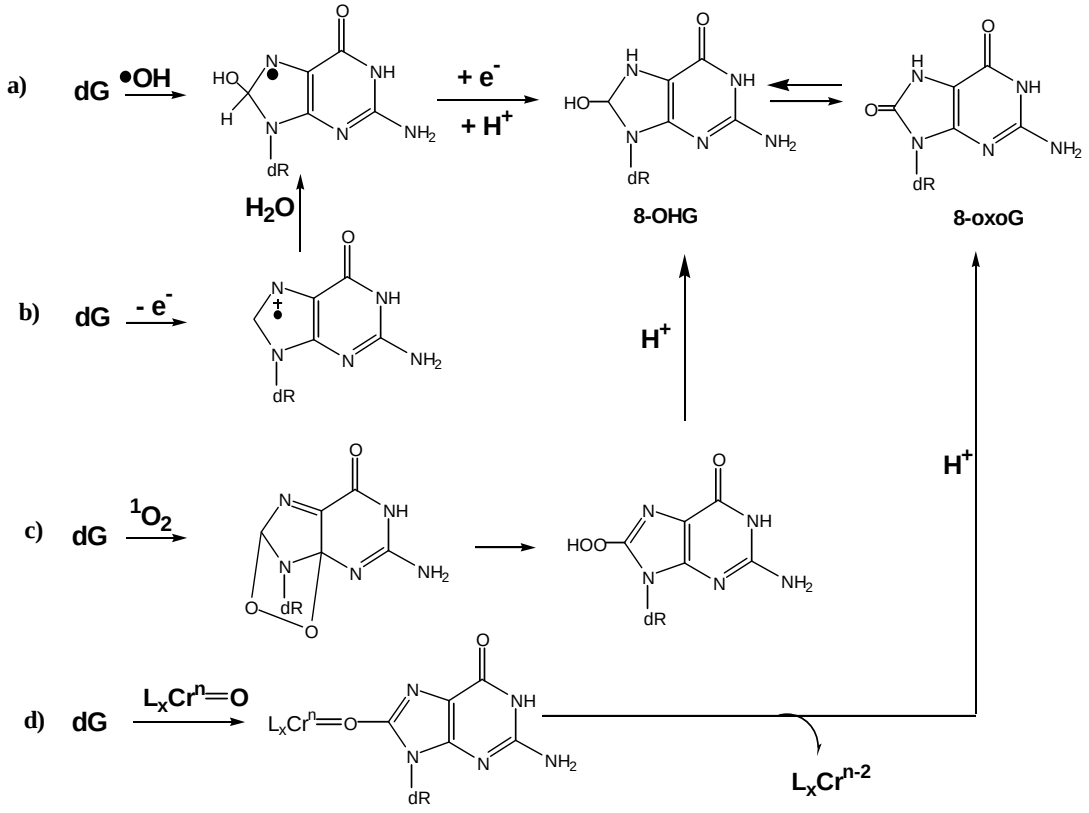

Figure 1.5 Multiple pathways of 8-oxoG formation by chromium or ROS [9].

1.3 Nucleosomal Chemical Damage

The *in vitro* cross-linking and oxidation of free DNA by numerous agents has been examined extensively in the literature. However, in eukaryotes nearly 80 % of nuclear DNA is wrapped around histones providing a significantly different DNA structural setting. Studies on nucleosomal DNA damage can be categorized into two schools of experimental approach. The first resembles an pseudo-*in vivo* approach whereby intact nucleosome structures were extracted from cells, treated and then examined. Such studies provided a general feeling for the effect of the nucleosome

setting but lacked the ability to probe in detail any mechanistic or structural effects of the NCP alone. Generally, such studies inferred regions of localized DNA damage, such as in linker DNA or in Nucleosomal regions. The second approach utilizes extracted histone proteins and a known sequence of DNA to create a reconstituted nucleosome core particle. The reconstituted NCP system allows for a detailed systematic study of the effect of the NCP on DNA processes. DNA fragments commonly used for reconstitution are a 154 bp fragment of the Xp-11 plasmid from the 5S rRNA gene of *X. borealis,* the 146 bp fragment from the *L. variegatus* 5S rRNA gene or the 134 bp fragment of the *S. cerevisiae* DED1 promoter (HISAT sequence) [41]. The use of these fragments for chemical modification studies has allowed accurate controls, cross comparisons, site directed (rotational and translational) and sequence specificity studies. The sequence of the Xp11 154 bp 5S rRNA gene fragment is ideal for oxidative damage studies with its high guanine content, numerous GC-CG base pair steps as well as a run of eight guanines that are coincident with the more deformed wrapping region of DNA, figure 1.6.

The chemical agents investigated with the 154 bp 5s rRNA gene have included Cu(II)/H_2O_2 and Fe(II)EDTA Fenton chemistry, protein crosslink studies utilizing cis and trans-diamminedichloroplatinum (II), nitrogen mustard family antitumor agents and benzo[a]pyrenediol epoxide. Additional agents such as bleomycin, neocarzinostatin, melphalan and UV light have been investigated using the *Xenopus laevis* and HISAT sequences. Collectively, reconstitution and pseudo-*in vivo* studies of nucleosomal DNA damage have exhibited a spectrum of effects compared to naked DNA ranging from protective, enhanced, and even no effect. The nucleosome protects DNA from damage from a diverse array of agents including bulky chemicals: N-acetoxy-2-

acetylaminofluorene [42], aflatoxin [43], benzo[alpha]pyrene diol epoxide [44, 45]; small alkylating agents: n-methyl-n-nitrosourea (MNU) [46]; ionizing radiation: γ-ray [47]; antitumor drugs: bleomycin, neocarzinostatin, and melphalan [48, 49]; cross-linking agents: cisplatin and its analogues [50], mitomycin C [51], trimethylpsoralen [52]; and Fe(II) Fenton generated radicals [53, 54]. No protective effect has been observed with agents such as UV radiation [55], dimethylsulfate [46, 56], and *cis*- and *trans*-diamminedichloroplatinum(II) [57]. One study to date, has shown increased DNA cleavage in the nucleosome with low concentrations of Cu(II) generated Fenton chemistry [58].

```
AATTCGAGCT CGCCCGGGGA TCCGGCTGGG CCCCCCCCAG AAGGCAGCAC
TTAAGCTCGA GCGGGCCCCT AGGCCGACCC GGGGGGGGTC TTCCGTCGTG

AAGGGGAGGA AAAGTCAGCC TTGTGCTCGC CTACGGCCAT ACCACCCTGA
TTCCCCTCCT TTTCAGTCGG AACACGAGCG GATGCCGGTA TGGTGGGACT

AAGTGCCCGA TATCGTCTGA TCTCGGAAGC CAAGCAGGGT CGGGCCTGGT
TTCACGGGCT ATAGCAGACT AGAGCCTTCG GTTCGTCCCA GCCCGGACCA

TAGT
ATCA
```

Figure 1.6 Sequence of the *Eco*RI-*Rsa*I restriction fragment of the *Xenopus borealis* 5S rRNA gene

All these studies have provided mixed results with regard to the localization of DNA damage in the NCP. However, given the nature of histones to dictate DNA region accessibility, different results would be expected depending upon the mechanism of modification, steric considerations and the area of localized attack. Nonetheless, correlations cannot be viewed as being ideally straightforward. Despite the altered state

of DNA in the nucleosome, long range charge transport can still occur [59]. Disruption of the integrity of nucleosome core particles by experimentation can also provide further discrepancies when conducting these studies. Such discrepancies are illustrated by the conflicting results of ciplatin damage observed between the Millard and Wilkes [57] and Galea and Murray studies [50].

The Cu(II)/H_2O_2 study by Liang and Dedon used reconstituted nucleosome core particles (formed from the 154 bp Xp11 fragment) as a model to examine the protective nature of the nucleosome against copper- and iron- mediated Fenton chemistry [58]. Rather than protection, an enhanced oxidation of nucleosomal DNA relative to naked DNA was generated by Cu(II) pseudo-Fenton chemistry at lower concentrations with a 2 fold increase in strand breaks and a 8 fold increase in base lesions sensitive to Fpg and EndoIII. In nucleosomal DNA oxidative damage of base lesions outnumbered strand breaks by a factor of 3-4 while in naked DNA the ratio of strand breaks to base lesions was 0.6. In both naked and NCP substrates damage to nucleobases was localized around regions of guanine abundance. While Fe(II)-EDTA hydroxyl radical studies exhibited a rotational footprint no apparent footprinting effect was seen in the nucleosome with copper Fenton chemistry. Explanations for these results were ascribed to the high affinity of Cu(II) for amines, which are highly concentrated on the surface of the histone, and an increased accessibility and reactivity due to DNA structural changes set forth by the nucleosome [58]. The question now is how will chromium interact with the NCP and what effect will the DNA structural changes set forth by the nucleosome have on chromium mediated DNA oxidation?

1.3.1 Chromium Mediated DNA Damage to Free and Nucleosomal DNA Substrates

The focus of this project is to study the effects of the nucleosome structure on chromium-induced DNA damage. Of particular interest is to determine if the translational and rotational setting and DNA perturbations set forth by the nucleosome will enhance or protect DNA against damage and dictate oxidative hot spots. In the process of reduction chromate exposure has illustrated the ability to attack through metal mediated and radical pathways, primarily attacking, respectively, the nucleobase or the deoxyribose [9]. It is expected that the distribution of nucleosomal DNA damage will depend upon the dominant mechanistic route. Chromate Fenton-like chemistry (using ascorbic acid and H_2O_2) will create hydroxyl and ascorbate radicals in addition to high valent chromium complexes [18]. It was our hypothesis that damage mediated by this mechanism will be mitigated in nucleosomal substrates and that a rotational dependence of oxidation would be observed with increased oxidation on DNA facing away from the histone surface. The high valent chromium complexes Cr(IV) and Cr(V) that are generated by the reduction of chromate by ascorbic acid are capable of oxidizing DNA through a metal mediated pathway [9]. Metal mediated oxidation as a result of chromate reduction was also expected to exhibit a damage pattern consistent with hindered access to DNA in the nucleosome. It was expected that metal-mediated oxidation would exhibit an increased rotational dependence relative to hydroxyl radical damage due to differences in accessibility. It was unclear how the affinity of high valent chromium(V) for the DNA phosphate backbone [60] would affect the propensity for strand breaks or nucleobase oxidation. However, it was believed that both mechanistic pathways would favor nucleobase damage over sugar damage in the nucleosomal setting due to increased

relative accessibility set forth by the nucleosome. Given the oxidative sensitivity of guanine that is enhanced within consecutive runs of guanines at the 5' of GG and GGG sequences, oxidation was expected to be localized to these regions. In addition, given the reduced size of the minor groove in the nucleosome, and increased accessibility to the N7 in the major groove of duplex DNA it was expected that the majority of nucleobase DNA damage would also be localized to guanine(s) in the major groove facing away from the histone surface.

1.4 Materials and Methods

1.4.1 Histone Extraction

All steps were done on ice or at 4 ^{o}C. Frozen chicken blood was thawed in 6% sodium citrate and clots were broken up with a loose fitting Dounce homogenizer. Samples were centrifuged at 2,000 x *g* for 10 min then resuspended in 15 mM sodium citrate and 150 mM NaCl. The nuclear pellet was frozen and thawed in a cell lysis buffer [100 mM Tris (pH 7.2), 150 mM NaCl, 0.5 mM PMSF], washed 4-5 times with 0.2% Igepal (Sigma) and the buffy coat was removed. Nuclei were ruptured with a nuclei lysis buffer [100 mM Tris (pH 7.8), 2 mM EDTA, 0.5 mM PMSF] and chromatin was pelleted by centrifugation at 16,000 x *g* for 30 min. Nucleosomal DNA was digested with 10,000 units of micrococcal nuclease (NEB) in 10 mM Tris (pH 7.8) and 1 mM $CaCl_2$ at room temperature for 1 hour with successive trituration with broken pasteur pipets of orifices ~4, 3, 2, and 1 mm. The digestion was stopped with the addition of EDTA to a final concentration of 2 mM. The sample was spun at 10,000 x *g* for 30 min and the pellet was discarded. H1 internucleosomal linker histones were removed by cation exchange by

stirring the supernatant with CM-Sephadex C-25 (30 mg/mL) with a slow NaCl gradient to a final concentration of 50 mM. After centrifugation at 10,000 x *g* for 10 min the resulting supernatant was collected and dialyzed overnight in a slide-alyzer cassette (Pierce 10,000 MWCO) against 20 mM Tris (pH 7.8), 0.2 mM EDTA. Following centrifugation at 10,000 x *g* for 10 min the supernatant was digested again with 10,000 units of micrococcal nuclease (NEB) in 10 mM Tris (pH 7.8) and 1 mM $CaCl_2$ at 37 ^oC for 30 min. The reaction was brought to 125 mM NaCl, placed on ice and stirred for 60 min. After centrifugation at 10,000 x *g* for 15 min the supernatant was dialyzed overnight against 20 mM Tris (pH 7.2), and 0.2 mM EDTA. Additional dialysis steps were done in 20 mM Tris (pH 7.2) to remove EDTA. The sample was lyophilized to dryness and relative protein concentration was determined using a BCA assay (Pierce, IL). The presence of histone protein was confirmed with an 18% SDS PAGE gel with Coomassie staining.

1.4.2 DNA Amplification

The Xp11 plasmid was obtained from Dr. Julie Millard at Colby College (ME). The plasmid was introduced by transformation into *E.coli* DH5α and grown in sufficient quantities using standard techniques [61]. Primers were designed to allow amplification of the 154 bp high affinity wrapping fragment. The reverse primer was purchased with a 5' phosphate group to allow for 5'-^{32}P labeling of only the forward strand. Amplified products were identified and purified from 1.2% Agarose gels using QIAex gel extraction kit (Qiagen). The following oligonucleotide primers were used in this study: Forward primer-5'-AAT TCG AGC TCG CCC, Reverse primer-5'-Phos- ACT AAC CAG GCC CGA

1.4.3 Substrate Preparation

DNA substrates were quantified using A_{260} absorbance values. DNA was 5'-^{32}P labeled with [γ-^{32}P] ATP (GM Healthcare) using 10 units of T4 polynucleotide kinase (T4 PNK, New England Biolabs) and 1x T4 PNK buffer at 37 ^{o}C for 40 min. Following labeling the oligonucleotides were purified using Micro Bio-Spin 30 (Biorad) columns.

1.4.4 Reconstitution

5'-^{32}P labeled 154 bp fragments were incubated with histone protein (0.8:1 molar ratio) in 1 M NaCl, 10 mM Tris (pH 7.2), and 1 mM PMSF (28 μL total volume) for 1 hr on ice. Aliquots of 10 mM phosphate, Tris-HCl or MOPS Buffer (pH 7.5) were added at 1 hour intervals to dilute the NaCl concentration in a stepwise manner to 0.8, 0.67, and 0.1 M NaCl. Free and nucleosomal DNA were separated on a 6% native PAGE gel (30.19:1, acrylamide/Bis) containing 5 % glycerol, and run in 0.5X TBE at 220 V for 20 min. Autoradiography was utilized to visualize reconstitution. Wrapping efficiency was determined by densitometry of the wrapped and unwrapped bands with Bio-Rad Quantity One software.

1.4.5 Cr(VI)/Ascorbate Damage

Ascorbic acid (>99%) and sodium dichromate were purchased from Sigma-Aldrich. The 154 bp free and nucleosomal DNA (1-7 μg) were treated with Cr(VI) and Ascorbate at ratios of 1:1, 1:5 and 1:10 respectively. Concentrations of Cr(VI) varied from 25-200 μM with ascorbate ratios of 10:1 to 1:1. Hydrogen peroxide when utilized, was added last at concentrations up to 500 μM. Treatments were carried out for 1 hour at room temperature.

1.4.6 Analysis of Site and Sequence-Specific Oxidation of DNA by Chromium

All DNA samples were purified by phenol:chloroform extraction followed by Micro Bio-Spin 6 or 30 chromatography columns (BioRad) or ethanol precipitation. Piperidine labile cleavage sites on the DNA were analyzed by treating purified lyophilized samples of the chromium treated DNA with 100 μL of a 1.0 M (10%) solution of freshly distilled piperidine followed by heating at 90 ^{o}C for 30 min. BER glycosylase labile sites were analyzed by enzymes Fpg or hOGG1 (NEB) under the enzyme suppliers recommended conditions, namely: 1x buffer 1 (NEB Fpg) or buffer 2 (NEB hOGG1), 1x BSA at 37 ^{o}C. Samples were loaded on a 8-15% (depending on focusing area) denaturing (7 M urea) polyacrylamide gel, 0.4 mm thickness, 21 cm × 50 cm. The gel was pre-warmed to 50 ^{o}C and lyophilized samples were loaded with a 80% formamide loading buffer containing 0.05% xylene cyanol and bromophenol blue, 1 mM EDTA, and 10 mM NaOH. Electrophoresis was carried out at 2300 V and 24 mA with 2X TBE as the running buffer. Visualization of the DNA cleavage products was carried out by autoradiography with a phosphoimager. Maxam-Gilbert G-A lanes were utilized to assign bands.

1.5 Results

1.5.1 Preparation of Nucleosome Core Particles

Histones were extracted from chicken erythrocytes as previously described by Millard et al., 1998 [51] and identified by SDS-PAGE, figure 1.7. The Xp11 plasmid was previously obtained from Julie Millard at Colby College and the plasmid was introduced into *E.coli* DH5α, grown in sufficient quantities and extracted using the QIAprep miniprep kit (Qiagen). After extraction the 154 bp high affinity wrapping

fragment was isolated with *EcoR*I/*Rsa*I double digest of the Xp11 plasmid followed by agarose gel purification of the 154 bp band. Polymerase chain reaction was eventually utilized to replace the inefficient restriction digest and extraction of the 154 bp wrapping fragment from the plasmid, figure 1.8. An additional advantage of PCR is that only one of the DNA strands can be easily labeled for Maxam-Gilbert sequencing. This can be done either by labeling the primer prior to carrying out PCR or by purchasing one primer with a 5' phosphate and carrying out blunt end labeling on the other strand following PCR.

Labeled DNA was purified with Micro Bio-Spin 6 (BioRad) columns and reconstituted into nucleosomes using the dilution technique as described by Millard and Wilkes [57]. The dilution technique is based on the principle of first dissociating the histone proteins and DNA at high salt concentration and then slowly reconstituting and 'freezing in' the constituted nucleosome core at low salt concentrations. Nucleosome formation was visualized by an upward gel shift from the free DNA control on a 6% native PAGE, figure 1.9. Reconstitution efficiencies of 90% or greater were typical and only reconstitution efficiencies of 85% or greater were utilized in subsequent oxidation experiments.

A)

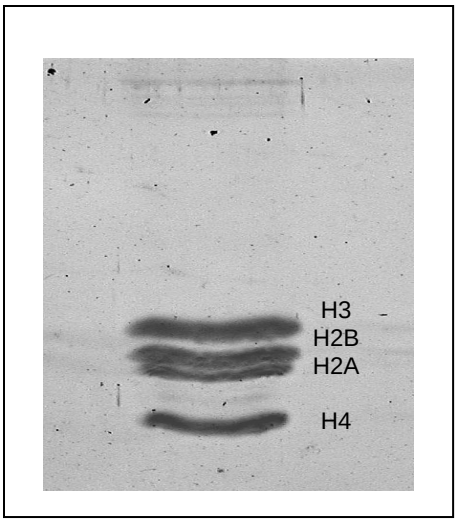

B)

Sub-unit	Molecular Weight	
H1	**21.5kDa**	**lysine rich**
H2a	**14.0kDa**	**slightly Lysine**
H2b	**13.8kDa**	**slightly Lysine**
H3	**15.3kDa**	**Arginine rich**
H4	**11.3kDa**	**Arginine rich**

Figure 1.7 SDS-PAGE gel of histone sub-unit separation A) Histone octamers isolated from chicken erythrocytes with H1 removed. B) Histone sub-units and corresponding molecular weight of calf thymus histones [62].

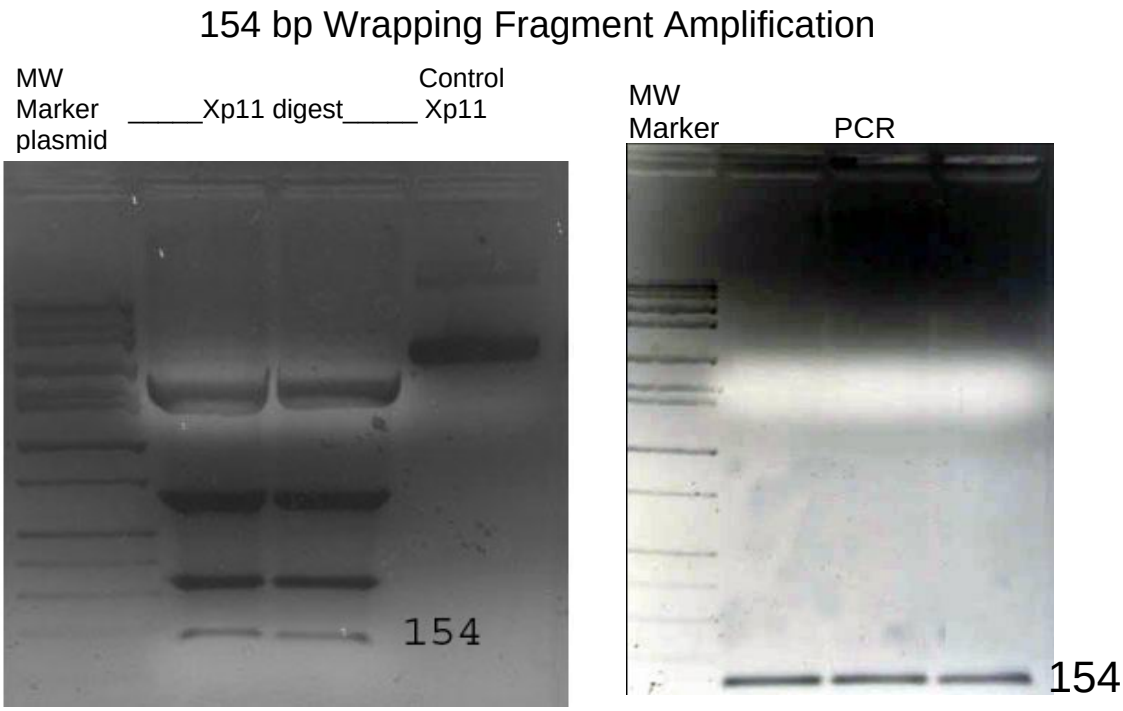

Figure 1.8 Agarose gel separation of 154 bp wrapping fragment from *Xenopus borealis* 5S rRNA gene. A) Plasmid *Eco*RI/*Rsa*I restriction enzyme digest production of 154 fragment; B) PCR production of 154 bp fragment.

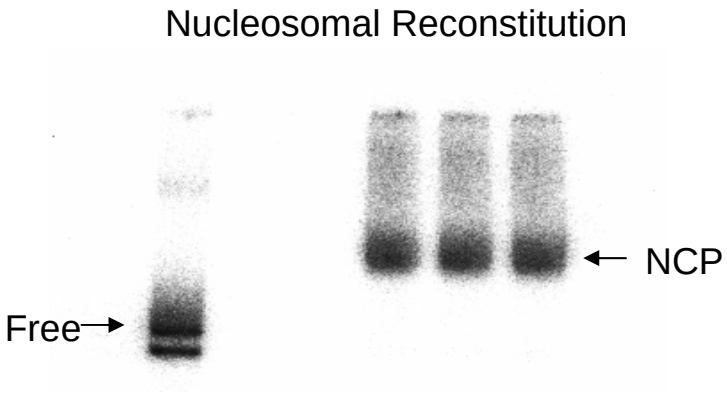

Figure 1.9 154 bp fragment of the *Xenopus borealis* 5S rRNA gene reconstituted into nucleosome core particles upon serial salt dilution in the presence of histone octamer, producing a characteristic gel shift in a native 5 % PAGE gel.

1.5.2 Analysis of Site and Sequence-Specific Oxidation of DNA by Chromium

To understand how chromatin structure affects chromate-mediated DNA damage, free and nucleosomal substrates were compared utilizing sequencing gel analysis. After the reconstitution of nucleosome core particles (NCP) were verified to be greater than 85%, free and NCP samples were subjected to conditions to mimic chromate metabolism while maximizing DNA oxidative damage. In attempt to visualize guanine nucleobase damage on sequencing gels, samples were treated with piperidine or base excision repair enzyme (BER) treatment by hOGG1 or Fpg. Only limited chromate oxidative damage was seen above background on free DNA or NCP samples and neither piperidine treatment nor BER glycosylase cleavage of damaged bases illustrated DNA damage above background. Cr(VI) and ascorbate reactions with the respective ratios of 1:1, 1:2.5, 1:5, 1:10 were used, in addition to studies using Cr(V)-salen, CR(V)-ehba and Cr(VI)- ascorbate and H_2O_2. While chromium-generated species produced little DNA

damage, positive controls of copper Fenton chemistry consistently produced intense DNA damage on sequencing gels.

Representative sequencing gels demonstrate no DNA damage above background in any samples of the 154 bp fragment in neither the free (figure 1.10) nor nucleosomal (figure 1.11, 1.12) substrates with the wide array of chromium treatment cocktails and piperidine nor BER cleavage treatment. Both forward and reverse primers were labeled in attempt to see the presence of oxidative damage above background. In addition to the variation in chromium treatment regimes, a variety of post treatment chromium salt cleanup techniques were utilized to investigate the possibility of lost damaged DNA in the clean-up step. These methods included Micro Bio-Spin 6 and 30 (BioRad) columns, ethanol and isopropanol precipitation and simple dilution. While it is still likely that these chromium generated lesions or adducts could cause unfavorable interactions and subsequent losses during clean up, copper Fenton chemistry positive controls were not problematic regardless of the cleanup technique utilized.

While chromium treatment regimes did not provide DNA damage above background, copper Fenton chemistry of free and nucleosomal samples produced similar amounts of DNA damage in a non sinusoidal footprint cleavage pattern, figure 1.12. Damage is most heavily localized at 5'guanines located in a run of two or more guanines as depicted by intense bands at G17, G24, G28, G43, and G47, figure 1.12. Little differences in site specificity, frequency or intensity of damage is seen between free and nucleosomal samples when treated at 100 μM Cu and 500 μM H_2O_2 . However, there are some regions of variable DNA damage and intensity around G40, G43 and the bands circled around bp 60 and 75, figure 1.12.

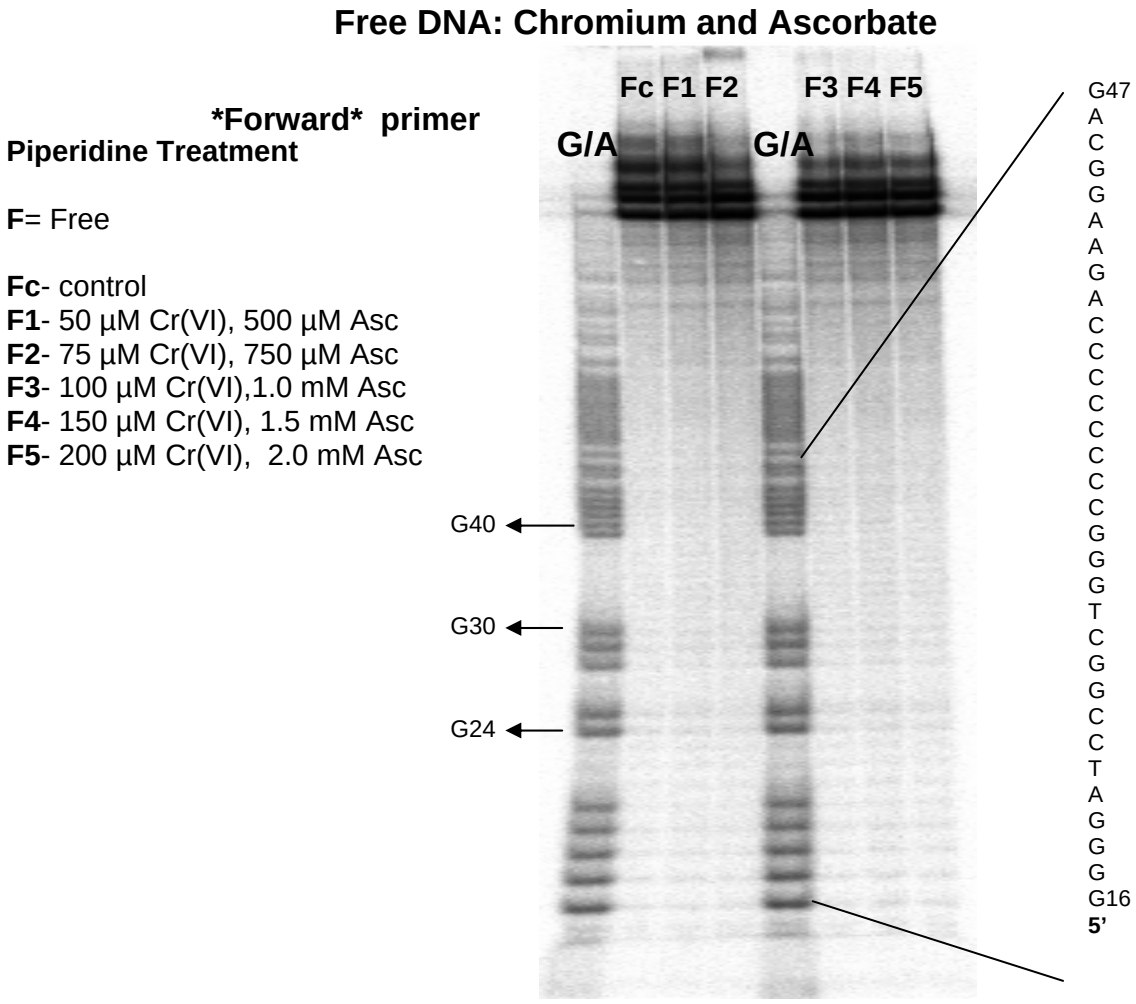

Figure 1.10 Sequence gel analysis of DNA damage produced by chromate and ascorbate upon treatment of free substrates of the forward 5' labeled 154 bp wrapping fragment. The "F" symbols represent free substrates. Lanes marked G/A represent Maxam-Gilbert chemical sequencing standard.

Free and Nucleosomal DNA: Chromium and Ascorbate

Reverse Primer

Piperidine Treatment
F= Free
N= Nucleosomal

Fc- Control
F1- 25 µM Cr(VI), 250 µM Asc
F2- 50 µM Cr(VI), 500 µM Asc
F3- 100 µM Cr(VI), 1 mM Asc

Nc- Control
N4- 25 µM Cr(VI), 250 µM Asc
N5- 50 µM Cr(VI), 500 µM Asc
N6- 100 µM Cr(VI), 1 mM Asc

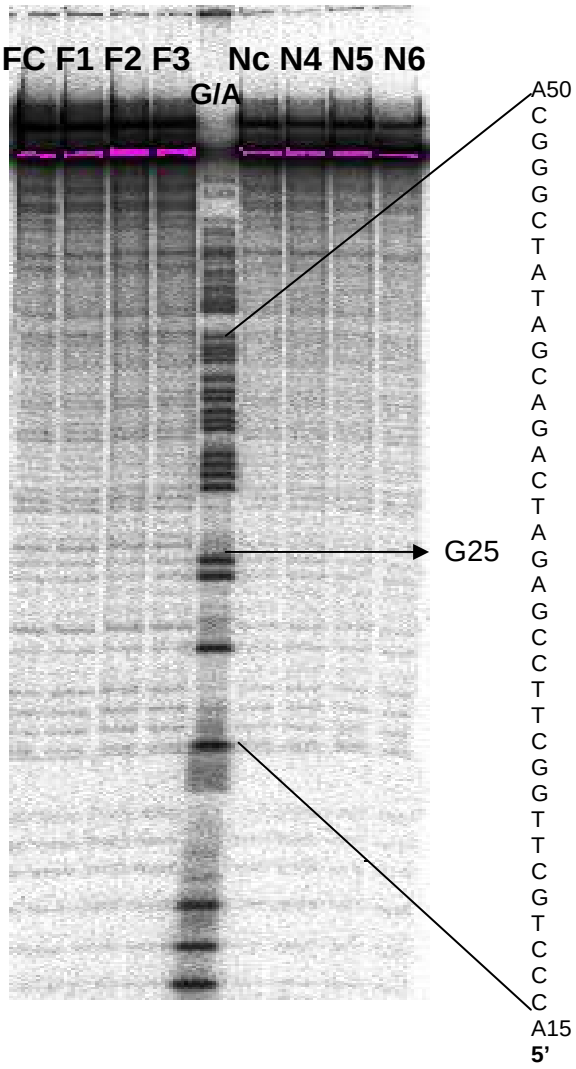

Figure 1.11 Sequence gel analysis of DNA damage produced by chromate and ascorbate upon treatment of free and nucleosomal substrates of the reverse 5' labeled 154 bp wrapping fragment. The "F" and "N" symbols represent, respectively, free and nucleosomal substrates. The Lane marked G/A represents Maxam-Gilbert chemical sequencing standard.

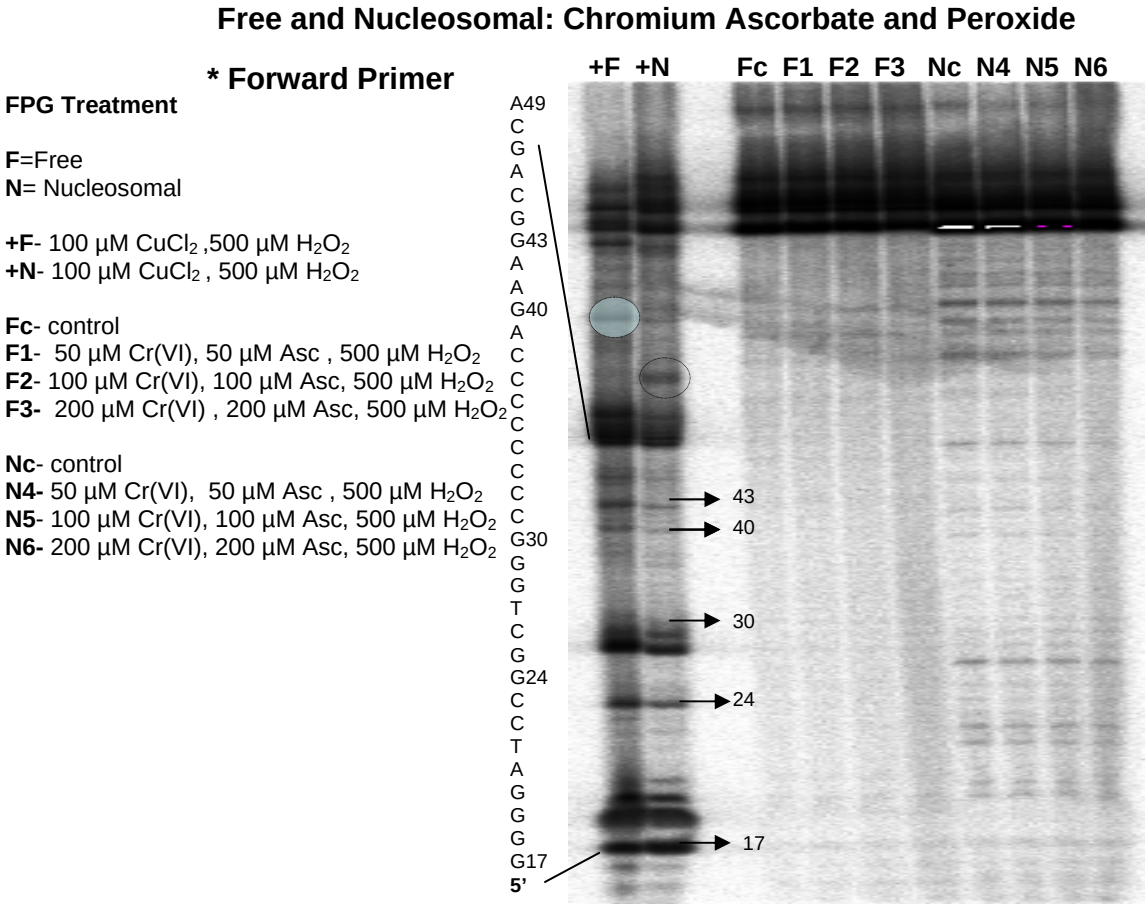

Figure 1.12 Sequence gel analysis of DNA damage produced by chromate, ascorbate and hydrogen peroxide upon treatment of free and nucleosomal substrates of the forward 5' labeled 154 bp wrapping fragment. The "F" and "N" symbols represent, respectively, free and nucleosomal substrates. The "+" symbol represents the positive control, 100 µM $CuCl_2$ and 500 µM H_2O_2. Numbers on right of first two lanes correspond to guanine bases counted from the labeled 5' end.

1.6 Discussion

The goal of this project was to better understand the mechanism of chromate-mediated oxidative damage in free and nucleosomal samples by visualizing oxidative hot spots on large sequencing gels and correlating damage to solution accessibility, oxidant mechanisms, steric considerations, and nucleosomal positioning. Unfortunately, chromate oxidative chemistry provided insufficient DNA oxidation to view with the techniques employed. Utilizing sequencing gel analysis previous studies in the field of chromate DNA damage have illustrated the potential for chromate to generate oxidized guanine lesions in small oligonucleotides [28, 63-65]. While identical chromate treatment procedures of these studies were followed, differences in sequence and length of the oligonucleotide could explain the lack of damage visualized in this study. These studies utilized smaller sequences of DNA, 22-28 base pairs [28, 63-65]. The fragment utilized in this study was 154 bp which provided a greater number of potential bases to be oxidized. In addition, given the significantly high GC content of the154 bp fragment this oligonucleotide has a greater ability to delocalize the damage.

The fact that copper Fenton chemistry consistently provided visual DNA damage suggests that the techniques and procedures in this study were done correctly. In addition, it illustrates that relative to copper Fenton chemistry, chromium is a weak oxidant. While only one copper concentration was utilized in this study, the results of copper induced DNA damage matches a previous study investigating copper DNA damage in the nucleosome [58]. Liang and Dedon (2001) observed that at lower concentrations of copper, nucleosomal DNA damage was augmented relative to naked DNA but as the copper concentration was increased past 75 μM DNA damage was

relatively similar in both settings with a limited footprint caused by the nucleosome [58]. This study observed similar results with copper-mediated DNA damage illustrating little difference in DNA damage in free and nucleosomal samples. DNA damage was mainly targeted at the 5'guanine in a series of adjacent guanines which is explained by the lowered redox potential of the 5'guanine. The lack of a protective footprint cleavage pattern in the nucleosomal substrates distinguishes the damage from Fe(II)-EDTA Fenton chemistry. While Cu(II) has illustrated a weak interaction with histones , 4-5 x 10^4 M^{-1} [66], this value is very similar to the estimated binding constant of Cu(II) to naked DNA, ~10^4 M^{-1} [67]. These results discredit the belief that Cu(II) histone binding explains the increase of Cu(II) Fenton generated DNA damage in the nucleosome. Instead, increased damaged to nucleosomal DNA may be attributed to copper species greater access and reactivity to nucleosomal DNA due to the DNA conformational changes associated with nucleosome formation.

While chromium DNA damage did not work in this study the foundation has been established to pursue other oxidants, or DNA processes in the nucleosomal setting. Future studies may entail the use of stronger oxidizing chromium complexes or the study of DNA methylation, DNA repair, and how epigenetic effects such as DNA methylation and histone acetylation can affect DNA process in the nucleosome.

1.7 References:

1. Wolfe, A., (2000) Chromatin: Structure and Function, 3rd Edition, Academic Press, NY.

2. Alberts, B., Johnson, A., Lewis, J., Raff, M., Roberts, K., Walter, P., (2001) Molecular Biology of the Cell, 4th edition, Garland Science, NY.

3. Richmond, T., Davey, C., (2003) The Structure of DNA in the Nucleosome Core, Nature. 423, 145-150.

4. Luger, K., Mader, A., Richmond, R., Sargent, D., Richmond, T., (1997) Crystal Structure of the Nucleosome Core Particle at 2.8 Å Resoltuion, Nature. 389, 251-260.

5. Hogan, M., Rooney, T., Austin, R., (1987) Evidence for Kinks in DNA folding in the Nucleosome, Nature. 328, 554-557.

6. Thåström, A., Lowary, P. T., Widom, J., (2003) Measurement of histone–DNA interaction free energy in nucleosomes. Methods. 33, 33–44.

7. Connett, P., Wetterhahn, K. E., (1983) Metabolism of the Carcinogen Chromate by Cellular Constituents. Structure and Bonding. 54, 93-124.

8. Martin, B. D., Schoenhard, J. A., Sugden, K. D., (1998) Hypervalent chromium mimics reactive oxygen species as measured by the oxidant-sensitive dyes 2',7'-dichlorofluorescein and dihydrorhodamine. Chem. Res. Toxicol. 11, 1402-1410.

9. Covino, J.J., Sugden, K., Genotoxicity of Chromate, Advances in Molecular Toxicology, 2 ed., Elsevier 2007.* (In Press)

10. Pratt, P. F., Myers, C. H., (1993) Enzymatic reduction of chromium(VI) by human hepatic microsomes, Carcinogenesis. 14, 2051-2057.

11. Jennette, K. W., (1982) Microsomal reduction of the carcinogen chromate produces chromium(V), J. Am. Chem. Soc. 104, 874-875.

12. Rossi, S. C., Gorman, N., Wetterhahn, K. E., (1988) Mitochondrial reduction of the carcinogen chromate: formation of chromium(V). Chem. Res. Toxicol. 1, 101–107.

13. Kawanishi, S., Inoue, S., Sano, S., (1986) Mechanism of DNA cleavage induced by sodium chromate(VI) in the presence of hydrogen peroxide. J. Biol. Chem. 261, 5952–5958.

14. Liu, K. J., Jiang, J., Goda, F., Dalal, N., Swartz, H.M., (1996) Low frequency electron paramagnetic resonance investigations on metabolism of chromium(VI) by whole live mice, Ann. Clin. Lab. Sci. 26, 176-184.

15. Stearns, D. M., Wetterhahn, K. E., (1994) Reaction of chromium(VI) with ascorbate produces chromium(V), chromium(IV), and carbon-based radicals. Chem. Res. Toxicol. 7, 219–230.

16. Stearns, D. M., Courtney, K. D., Giangrande, P. H., Phieffer, L. S., (1994) Wetterhahn, K. E., Chromium(VI) reduction by ascorbate: role of reactive intermediates in DNA damage in vitro. Environ. Health Perspect. 102, 21–25.

17. Stearns, D. M., Kennedy, L. J., Courtney, K. D., Giangrande, P. H., Phieffer, L. D., Wetterhahn, K. E., (1995) Reduction of chromium(VI) by ascorbate leads to chromium-DNA binding and DNA strand breaks in vitro. Biochemistry. 34, 910–919.

18. Shi, X., Mao, Y., Knapton, A. D., Ding, M., Rojanasakul, Y., Gannett, P. M., Dalal, N., Liu, K., (1994) Reaction of Cr(VI) with ascorbate and hydrogen peroxide generates hydroxyl radicals and causes DNA damage: role of a Cr(IV)-mediated Fenton-like reaction. Carcinogenesis. 15, 2475-2478.

19. Quievryn, G., Peterson, E., Messer, J., Zhitkovich, A., (2003) Genotoxicity and mutagenicity of chromium(VI)/ascorbate-generated DNA adducts in human and bacterial cells. Biochemistry. 42, 1062-1070.

20. Aiyar, J., Berkovits, H. J., Floyd, R. A., Wetterhahn, K. E., (1991) Reaction of chromium(VI) with glutathione or with hydrogen peroxide: identification of reactive intermediates and their role in chromium(VI)-induced DNA damage. Environ. Health Perspect. 92, 53–62.

21. Bose, R. N., Moghaddas, S., Gelerinter, E., (1992) Long-lived chromium(IV), chromium(V) metabolites in the chromium(VI)-glutathione reaction: NMR, ESR, HPLC, and kinetic characterization. Inorg. Chem. 31, 1987-1994.

22. Wiegand, H. J., Ottenwalder, H., Bolt, H. M., (1984) The reduction of chromium(VI) to chromium(III) by glutathione: An intracellular redox pathway in the metabolism of the carcinogen chromate. Toxicology. 33, 341-348.

23. Aiyar, J., Borges, K.M., Floyd, R. M.. Wetterhahn, K. E., (1989) Role of chromium(V), glutathione thiyl radical, and hydroxyl radical intermediates in chromium(VI) induced DNA damage. Toxicol. Environ. Chem. 22, 135-148.

24. Connett, P., Wetterhahn K. E., (1985) In vitro reaction of the carcinogen chromate with cellular thiols and carboxylic acids. J. Am. Chem. Soc. 107, 4282-4285.

25. Werfel, U., Langen, V., Eickhoff, I., Schoonbrood, J., Vahrenholz, C., Brauksiepe, A., Popp, W., Norpoth, K., (1998) Elevated DNA single-strand breakage frequencies in lymphocytes of welders exposed to chromium and nickel. Carcinogenesis. 19, 413–418.

26. Cantoni, O., Costa, M., (1984) Analysis of the induction of alkali sensitive sites in DNA by chromate and other agents that induce single strand breaks. Carcinogenesis. 5, 1207-1209.

27. Hamilton, J. W., Wetterhahn, K. E., (1986) Chromium(VI)-induced DNA damage in chick embryo liver and blood cells in vivo. Carcinogenesis. 7**,** 2085–2088.

28. Bose, R. N., Moghaddas, S., Mazzer, P. A., Dudones, L. P., Joudah, L., Stroup, D., (1999) Oxidative damage of DNA by chromium(V) complexes: relative importance of base versus sugar oxidation. Nucl. Acids Res. 27, 2219-2226.

29. Sugden, K. D., Wetterhahn, K. E., (1997) Direct- and hydrogen peroxide induced-chromium(V) oxidation of deoxyribose in single-stranded and double-stranded calf thymus DNA. Chem. Res. Toxicol. 10, 1397-1406.

30. Sugden, K. D., (1999) Formation of modified cleavage termini from the reaction of chromium(V) with DNA. J. Inorg. Biochem. 77**,** 177–183.

31. Robison, S. H., Cantoni, O., Costa, M., (1984) Analysis of metal-induced DNA lesions and DNA-repair replication in mammalian cells. Mutat. Res., 131, 173-182.

32. Pratviel, G., Bernadou, J., Meunier, B., (1995) Carbon-hydrogen bonds of sugar units as targets for chemical nucleases and drugs. Angew. Chem. Int. Ed. Engl. 34, 746-769.

33. Ames, B. N., Shigenaga, M. K., Hagen, T. M., (1993) Oxidants, antioxidants and the degenerative disease of aging. Proc. Natl. Acad. Sci. U.S.A. 90, 7915-7922

34. Kasai, H., Nishimura, S., (1991), Oxidative Stress: Oxidants and Antioxidants. by Sies, H, eds., Academic Press, Ltd, London, 99-116.

35. Beckman, K. B., Ames, B. N., (1997) Oxidative decay of DNA, J. Biol. Chem. 272, 19633-19636.

36. Ames, B. N., Saul, R. L., (1987) Oxidative DNA damage, cancer and aging. Ann. Intern. Med. 107, 526-545.

37. Steenken, S., Jovanovic, S.V., (1997) How easily oxidizable is DNA? One-electron reduction potentials of adenosine and guanosine radicals in aqueous solutions. J. Am. Chem. Soc. 119, 617-618.

38. Saito, I., Takayama, M., Sugiyama, H., Nakatani, K., (1995) Photoinduced DNA cleavage via electron transfer: Demonstration that guanine residues located 5' to guanine are the most electron donating sites. J. Am. Chem. Soc. 117, 6406-6407.

39. Steenken, S., Jovanovic, S. V., Bietti, M., Bernhard, K., (2000) The trap depth (in DNA) of 8-oxo-7,8-dihydro-2'-deoxyguanosine as derived from electron-transfer equilibra in aqueous solution. J. Am. Chem. Soc. 122, 2372-7234.

40. Bose, R. N., Fonkeng, B., Barr-David, G., Farrell, R. P., Judd, R. J., Lay, P. A., Sangster, D. F., (1996) Redox potentials of chromium(V)/(IV), -(V)/(III), and (IV)/(III) complexes with 2-ethyl-2-hydroxybutanoato(2-/1-) ligands. J. Am. Chem. Soc. 118, 7139-7144.

41. Smerdon, M. J., Thoma, F. (1998) Modulations in Chromatin Structure During DNA Damage Formation and DNA Repair. In: DNA Damage and Repair, Volume II: DNA Repair in Higher Eukaryotes, Nickoloff, J. A., and Hoekstra, M. F., eds., Humana Press Inc., Totowa, NJ, 199-222.

42. Lang, M. C., deMurcia, G., Mazen, A., Fuchs, R. P., Leng, M., Duane, M., (1982) Non-random binding of N-acetoxy-N-2-acetylaminofluourene to chromatin subunits as visualized by immunoelectron microscopy. Chem-Biol. Interactions. 41, 83-93.

43. Moyer, R., Marien, K., Holde, K. V., Bailey, G., (1989). Site-specific aflatoxin B1 adduction of sequence-positioned nucleosome core particles. J.Biol. Chem. 264, 226-231.

44. Smith, B. L., Macleod, M. C., (1993) Covalent binding of the carcinogen benzo[a]pyrenediol epoxide to Xenopus laevis 5S DNA reconstituted into nucleosomes. J. Biol. Chem. 268, 620-629.

45. Thrall, B. D., Mann, D. B. Smerdon, M. J. Springer, D. L., (1994) Nucleosome structure modulates benzo[a]pyrenediol epoxide adduct formation. Biochemistry. 33, 2210-2216.

46. Berkowitz, E. M., Silk, H., (1981) Methylation of chromosomal DNA by 2 alkylating-agents differing in carcinogenic potential. Cancer Lett.12, 311–321.

47. Chiu, S. M., Oleinick, N. L., (1982) Resistance of nucleosomal organization of eucaryotic chromatin to ionizing radiation. Radiat Res. 91, 516-532.

48. Smith, B. L., Bauer, G. B., Povirk, L. F., (1994) DNA damage induced by bleomycin, neocarzinostatin, and melphalan in a precisely positioned nucleosome-asymmetry in protection at the periphery of nucleosome-bound DNA. J. Biol. Chem. 269, 587-594.

49. Kuo, M. T., Hsu, T. C., (1978) Bleomycin causes release of nucleosomes from chromatin and chromosome. Nature. 271, 83-84.

50. Galea, A. M., Murray, V., (2002) The interaction of cisplatin and analogues with DNA in reconstituted chromatin. Biochimica et Biophysica Acta (BBA)/Gene Structure and Expression. 1579, 142-152.

51. Millard, J., Spencer, R., Hopkins, P., (1998) Effect of Nucleosome Structure on DNA Interstrand Cross-Linking Reactions. Biochemistry. 37, 5211-5219.

52. Conconi, A., Losa, R., Koller, T. H., Sogo, J. M., (1984) Psoralen-crosslinking of soluble and of H1-depleted soluble rat liver chromatin. J. Mol. Biol. 178, 920-928.

53. Ljungman, M., Hanawalt, P., (1992) Efficient protection against oxidative DNA damage in chromatin, Molecular Carcinogenesis. 5, 264-269.

54. Enright, H., Miller, W., Hebbel, R., (1992) Nucleosomal histone protein protects DNA from iron-mediated damage. Nucleic Acids Research. 20, 3341-3346.

55. Niggli, H., Cerutti, P., (1982) Nucleosomal distribution of thymine photodimers following far-and near-ultraviolet irradiation. Biochem. Biophys.Res. Commun. 105, 1215-1223.

56. Mcghee, J. D., Felsenfeld, G., (1979) Reaction of nucleosome DNA with dimethylsulfate. Proc. Natl. Acad. Sci. USA, 76, 2133-2137.

57. Millard, J., Wilkes, E., (2000) Cis and Trans-Diamminedichloroplatinum(II) Interstrand Cross-Linking of a Defined Sequence Nucleosomal Core Particle. Biochemistry. 39, 16046-16055.

58. Liang, Q., Dedon, P., (2001) Cu(II)/H_2O_2- Induced DNA Damage is Enhanced by Packaging of DNA as a Nucleosome, Chem. Res. Toxicol. 14, 416-422.

59. Nunez, M., Noyes, K., Barton, J., (2002) Oxidative Charge Transport through DNA in Nucleosome Core Particles, Chemistry & Biology. 9, 403-415.

60. Sugden, K., Wetterhahn, K., (1996) EPR evidence for chromium(V) binding to phosphate and pyrophosphate: implications for chromium(V)-DNA interactions. Inorganic Chemistry. 35, 3727-3728.

61. Current Protocols in Molecular Biology, Volume I. Ausubel, F., Brent, R., Kingston, R., Moore, D., Seidman, J., Smith, J., Struhl, K., eds., John Wiley & Sons. New York, 1990.

62. Johns, E. W., (1964) Studies on histone: Preparative methods for histone fractions from calf thymus. Biochem. J. 92, 55-59.

63. Slade, P. G., Hailer, M. K., Martin, B.D., Sugden, K.D., (2005) Guanine-specific oxidation of double stranded DNA by Cr(VI) and ascorbic acid forms spiroiminodihydantoin and 8-oxo-2'-deoxyguanosine. Chem. Res. Toxicol. 18, 1140-1149.

64. Sugden, K. D., Martin, B. D., (2002) Guanine and 7,8-dihydro-8-oxo-guanine-specific oxidation in DNA by chromium(V). Environ. Health Perspec. 110, 725-728.

65. Sugden, K. D., Campo, C. K., Martin, B. D., (2001) Direct oxidation of guanine and 7,8-dihydro-8-oxoguanine in DNA by a high-valent chromium complex: A possible mechanism for chromate genotoxicity. Chem. Res. Toxicol. 14, 1315-1322.

66. Gelagutashvili, E. S., Sigua, K. I., Sapojnikova, N. A., (1998) Binding and the nature of Cu(II) ion interaction with nucleosomes. J. Inorg. Biochem. 70, 207-210.

67. Bach, D., Miller, I. R., (1967) Polarographic investigation of binding of Cu^{2+} and Cd^{2+} by DNA. Biopolymers. 5, 161-172.

Chapter 2: Repair in the Nucleosome

2.1 Introduction: Nucleosomal DNA Repair

Eukaryotic DNA is packaged in a condensed state with histone proteins. The formation of the nucleosome core particle (NCP) introduces DNA structural changes providing a very different setting than that commonly modeled with *in vitro* studies [1]. These effects must be considered in any biochemical study in which DNA is a substrate. In general, interactions requiring multiple nucleotide interactions have been found to be significantly reduced in the nucleosomal setting [2]. Overall structural changes set forth by the NCP have illustrated restricted access to wrapped DNA by recognition proteins [3-5], repair enzymes [7-14], polymerases [6-8], restriction enzymes [1,7], nucleases [1,15-16] and many oxidizing and cross-linking agents [17-23]. Nucleosomal structural changes to DNA have also been shown to direct accessibility to certain translation and rotational regions of the NCP [1,8,24-25]. Cellular systems have developed several strategies to lessen the impediments associated with the nucleosome and chromatin to allow better access by polymerases, repair enzymes, transcription factors and other proteins involved in DNA processes. These strategies include histone post-translational modifications and ATP-dependent nucleosome remodeling [1].

In terms of DNA damage NCP studies have illustrated protective, enhanced, and no effect compared to naked DNA studies and the effects appears to be related to the type of oxidant, particularly its sterics, and interactions with the highly electropositive histone surface and altered DNA structure [17-23,26-27]. While there appears to be differences in efficiencies of oxidation of nucleobases in the nucleosomal setting and respective higher order nucleosomal structures, nucleobase oxidation is still widespread throughout

the genome. To combat global oxidation, DNA repair processes are required to work within or around this structural nucleosomal setting.

DNA oxidation is a common event that can be caused by a number of endogenous and exogenous factors and the DNA repair processes that repair it are crucial to cell survival. The two major cellular repair mechanisms that remove DNA damage are base excision repair (BER) and nucleotide excision repair (NER). The NER pathway is a complex biochemical process involving multiple large protein complexes (up to 30) which cooperate in a rapid sequential assembly mechanism to facilitate NER [28-32]. NER machinery handles a vast array of DNA lesions with varied structures. It has been postulated that NER doesn't recognize individual structures but specific conformational features [33]. While not completely understood, it appears that NER repair shows enhanced activity towards bulky DNA lesions that cause perturbations to DNA topology and or lesions that cause disruption of DNA base pairing [33-34]. The differences in repair rates by NER have been ascribed to local conformation flexibility surrounding the lesion [34] and the thermodynamic stability of the DNA adducts [33-36].

The BER pathway appears to be a simpler process involving the concerted activity of only a few proteins which catalyze individual reactions within the pathway. The BER family is involved in repairing small lesions that don't effect DNA topology and in many cases have only slight structural differences to their respective parent nucleobases. These lesions include 8-oxoguanine(8-oxoG), 8-hydroxyadenine(8-oxoA), foramidopyrimidine (Fapy) guanine (FapyG), Fapy-adenine (FapyA) and methyl-Fapy-guanine, 5-hydroxy-uracil (HOU), 5-hydroxy-cytosine (HOC), aflatoxin B1-Fapy-guanine, and spiroiminodihydantoin (Sp) to name a few. The variety of small lesions

cleaved by the BER family is a result of the variety of different BER glycosylases and their ability to repair multiple lesions [37]. hOGG1 for example can recognize and cleave 8-oxoG, 8-oxoA, FapyG and FapyA.

The BER pathway occurs in two steps. The first step is recognition by a BER family glycosylase that subsequently removes the damaged base producing a shared product of all BER glycoylases independent of the lesion, an abasic site (AP) [38-39]. After this initial step two phases of BER can be undertaken, short patch BER or long patch BER. Both pathways involve the removal of the abasic site but only one pathway replaces the damaged base (short-patch BER) while the other replaces the damaged base in addition to 2-13 adjacent bases (long-patch BER). The second step in short patch BER involves the removal of the AP site by an AP endonuclease, replication by Polβ/XRCC1 and DNA ligation with DNA ligase I, or Ligase III/XRCC1. Long patch BER differs in that it utilizes Pol β, δ or ε in conjunction with PCNA to produce a 2-13 bp patch that displaces the damaged strand. Subsequently, the extending flap is removed by FEN1 and the resulting nick is ligated with DNA ligase I [40-41].

Although BER and NER have significant differences in repair mechanisms they both have to deal with a DNA substrate that is far from the "naked" form in which they are commonly studied *in vitro*. *In vivo* DNA exists as chromatin forcing the repair machinery of NER and BER to deal with a distorted DNA structure and reduced accessibility due to the bulky histone proteins and superhelical wound DNA. To date a handful of studies have employed *in vitro* reconstitution of nucleosome core particles (NCP) to investigate the effects of nucleosomal DNA on the repair efficiency of both NER and BER machinery.

NER repair studies in the nucleosome have given insight into the cooperative process involved in repair in the nucleosome. Given the number of bulky proteins that cooperate to form the NER machinery, the large excised DNA fragments, and DNA helix distortion NER produces, it is believed that NER repair occurs in regions absent of the histone protein [31,32, 42,43]. Early observations by Michael Smerdon have pointed towards the phenomenon of specific nucleosomal rearrangements prior to excision repair [43]. To date numerous studies have provided further evidence of this rearrangement process (See ref 32 & 42 for good NER reviews). A widely accepted mechanism for NER has been termed the "access-repair-restore" mechanism in which damage is detected, chromatin is remodeled, the damage is made accessible by NER machinery and the site is excised and the nucleosome is restored [44-45]. Such remodeling explains the reduced NER efficiency seen in the nucleosome with *in vivo* and *in vitro* repair assays [12,13, 46-48].

In parallel to the helix distortion caused by the NER mechanism, crystal studies of BER glycosylases in action have illustrated that the targeted base is flipped out (to facilitate excision) producing significant global DNA distortion [49-51]. This is best illustrated by the crystal structure (2NOB) of hOGG1 glycosylase in action, figure 2.1 and 2.2. Four structural super families of DNA glycosylases have been identified so far , UDG (uracil DNA glycosylase), AAG (alkyladenine DNA glycosylase), MutM/Fpg (bacterial 8-oxoguanine DNA glycosylase) and HhH-GPD (hOGG1). While each super family is structurally discernible they all share the same extrahelical cleavage mechanism. This mechanism entails binding primarily to the lesion-containing DNA strand, recognizing the lesion and kinking the DNA to help flip the lesion out into the

active site pocket of the enzyme [52]. Once in the active site the lesion is released through cleavage of the glycosidic bond (C1'), figure 2.3. The extrahelical mechanism is advantageous for it allows better access to the sugar moiety and provides a better working environment by excluding water [50]. The need for the extrahelical mechanism is exemplified by the mechanism of Fpg and hOGG1 in which access to the C1' on the deoxyribose is required for nucleophilic attack by the amino group of lysine and subsequent release of the lesion, figure 2.3. Given the DNA distortion caused by DNA glycoylases the question that remains unanswered is whether *in vivo* BER utilizes a similar "access-repair-restore" mechanism as NER or if the smaller BER machinery carries out repair on the nucleosome with out the repositioning of the nucleosome.

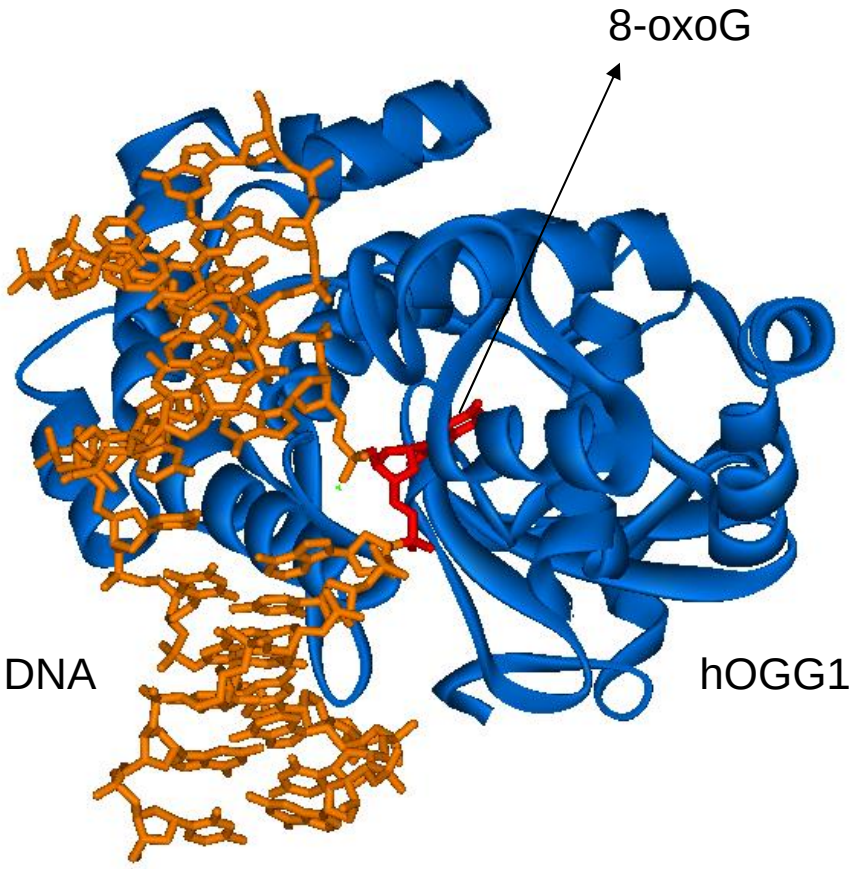

Figure 2.1- Crystal structure of hOGG1 activity on a DNA substrate containing an 8-oxoG lesion. DNA is represented in orange, hOGG1 in blue, and 8-oxoG in red. Image was created using Viewerlite and PDB crystal 2NOB [53].

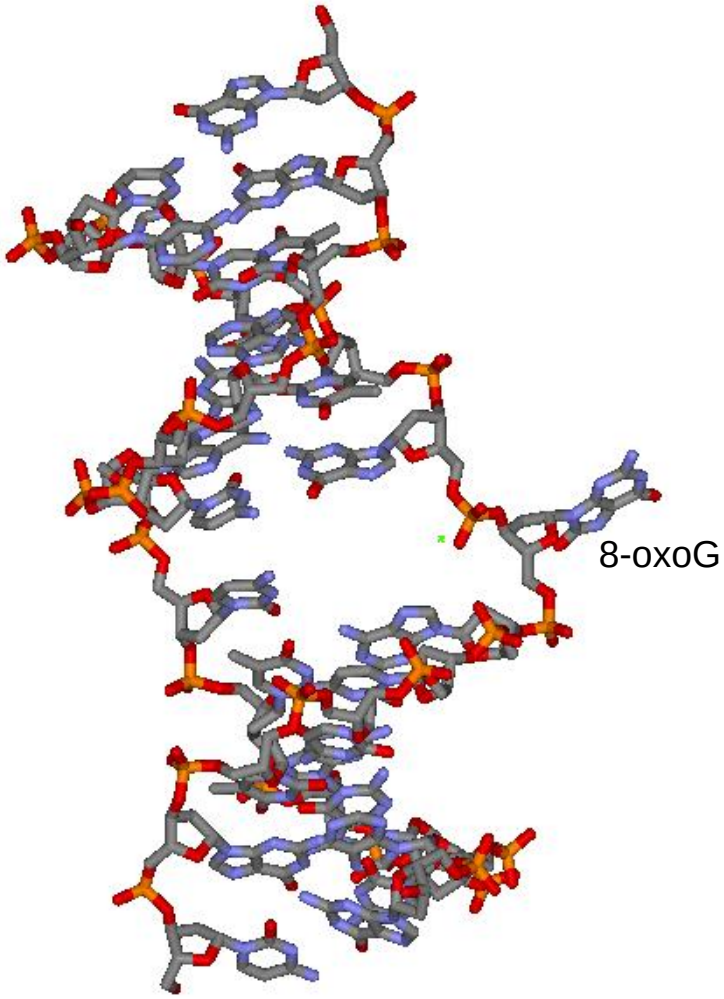

Figure 2.2- Crystal structure of hOGG1 activity on a DNA substrate containing an 8-oxoG lesion with the protein omitted. Image was created using Viewerlite and PDB crystal 2NOB [53].

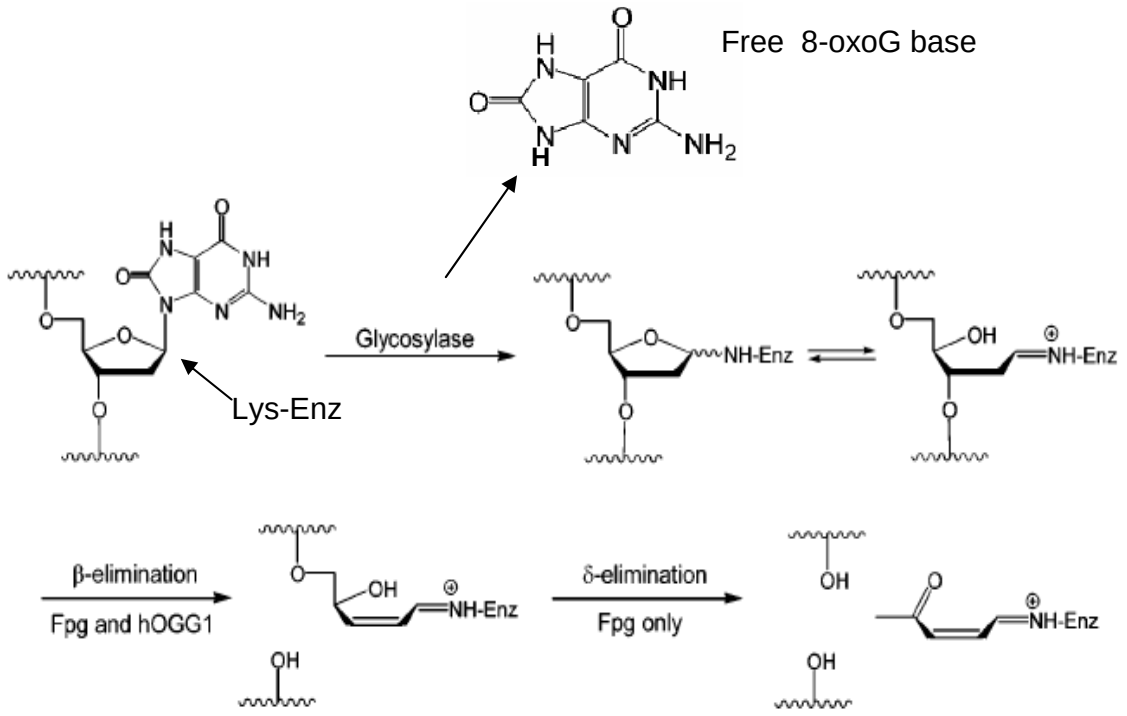

Figure 2.3- Fpg and hOGG1 mechanism of excision of 8-oxoG. Modified from mechanism by Hamm et al, 2007 [54].

A few *in vitro* studies have been conducted with mono-NCP to assess the effect of histones on BER repair. The majority of these studies focused on the BER enzymes associated with the repair of uracil residues produced from the deamination of cytosine or the misincorporation of dUMP opposite adenine (A) residues during replication. Nilsen et al. (2002) examined the excision rates of two major mammalian uracil DNA glycosylase UNG2 and SMUG1 of a U:A bp positioned at different locations on a NCP wrapped fragment (146 bp 5S rRNA L*ytechinus variegatus*) reconstituted with histones purified from chicken erythrocytes [7] . Overall, enzyme cleavage assays illustrated a 3-9 fold reduction in uracil removal from nucleosomal substrates with no rotational dependence on the three different uracil sites [7]. The presence RPA and PCNA were shown to have no effect on the repair process in the nucleosomal setting despite the fact

that these proteins are known to interact with UNG2 during repair [7]. Furthermore, efficient strand incision was seen with APE1 (abasic site removal) on NCP substrates and although activity was reduced, Pol β was able to extend one nucleotide on nucleosomal substrates [7]. In a similar study, Beard et al. 2003 investigated uracil removal and repair (G:U) in reconstituted NCP with UDG, APE1 and Pol β. The study found the activity of UDG in the nucleosome to be reduced by a factor of ten but saw a rotational dependence on repair with uracil residues facing away from the histone octamer exhibiting 2-3 times faster excision than those facing the octamer [8]. In disagreement with Nilsen et al. (2002) this study found complete inhibition of Polβ in the nucleosomal setting [8]. A complementary study by Beard et al (2005) found that removal of histone tails (by trypsin digest) did not affect DNA-histone reconstitution nor the activity of BER enzymes, UDG, APE1 or Polβ [9].

A number of *in vitro* studies have also been done to investigate the efficiencies of BER enzymes DNA ligase I and FEN1 in the nucleosome. Chafin et al (2000) examined DNA ligase I activity on reconstituted NCP with the *X. borealis* 5S rRNA gene wrapping fragment. Results indicated that ligase activity was reduced 4-6 fold on either side of the dyad while a 10 fold reduction was observed at the dyad [55]. Kysela et al. (2005) indicated that DNA ligase IV in conjunction with XRCC4 can ligate nucleosomal substrates at similar efficiencies to free substrates. However, when H1 was added the activity of the enzyme complex was found to be significantly inhibited in both free and NCP substrates [56]. Of all the studies done only one has shown increased enzyme efficiency in nucleosome substrates. Huggins et al. (2002) illustrated that FEN1 repair of flaps (mimicking long patch BER) had a 1.3-7 fold higher efficiency for nucleosomal

substrates at lower enzyme concentrations. In addition, histone tails appeared to increase cleavage suggesting a beneficial binding interaction [57]. In summarizing these results it appears that BER in the nucleosomal setting requires more research with further emphasis on histone post-translational modifications, H1 and histone tails, and their implications to BER repair. Furthermore, while there are a number of BER glycosylases, only UDG and SMUG1 glycosylase activities have been investigated in the nucleosomal setting (see Reference 41 for a comprehensive review on BER repair in the nucleosome).

To date no work has been done on the repair of 8-oxoG in the nucleosomal setting despite the fact that 8-oxoG is the lesion that has historically been associated with DNA nucleobase oxidation. 8-oxoG has been shown to form from a variety of redox active xenobiotics and endogenous metabolic processes including chromate exposure. It has been estimated that 8-oxoG occurs at a frequency of ~10,000 bp per cell per day [58]. Because of the high frequency of occurrence, 8-oxoG has been implicated in the etiology of a large number of diseases and has been extensively used as a sensitive biomarker for oxidative damage to the cell [59-61]. Cellular repair of 8-oxoG is imperative to preventing cellular mutagenesis and toxicity. 8-oxoG is repaired by the BER pathway with a variety of BER glycosylases illustrating the ability to bind and cleave this lesion. hOGG1 (human) and Fpg (bacterial) are considered to be the dominant glycosylases for 8-oxoG.

It is well known that hOGG1 and Fpg repair the 8-oxoG lesion when paired opposite cytosine, thymine or guanine in double stranded DNA [62]. As illustrated, these glycosylases excise oxidized lesions with the formation of a Schiff base intermediate between the primary amine of the glycosylase and the C1' of the deoxyribose, figure 2.3

[54]. While both hOGG1 and Fpg exhibit lyase activity, recent studies have illustrated the stimulation of glycosylase activity with the addition of human AP Endonuclease, APE (also known as HAP1) [63]. hOGG1 has illustrated inefficient AP lyase activity with a low turnover rate. The addition of APE1 appears to bypass this rate limiting step of hOGG1 lyase activity and increase base excision activity [63]. Unpublished results in this lab have indicated a similar effect on Fpg glycosylase activity. This cooperative effect explains the need for APE1 in cellular systems despite the fact that many glycosylases have lyase activity. Furthermore, it suggests that BER cleavage assays should employ the use of APE1 to better mimic the *in vivo* workings of BER and allow the glycosylases to carry out their primary function. This phenomenon also raises new questions about the possibility of further cooperativity between BER machinery.

The focus of this study is to investigate the cleavage efficiencies of hOGG1 and Fpg on free and nucleosomal 8-oxoG substrates. By placing an 8-oxoG lesion in different nucleosomal rotational settings this study will also examine the ability of Fpg and hOGG1 to deal with altered lesion accessibility in the nucleosome. Of particular interest is if *in vivo* BER utilizes a similar "access-repair-restore" mechanism as NER or if the smaller BER machinery carries out repair on the nucleosome without the need for nucleosomal repositioning?

2.2 Materials and Methods

2.2.1 Histone Extraction

The procedure was identical to that described in Chapter 1, Section 1.4.1.

2.2.2 DNA Substrates

The procedure was identical to that described in Chapter 1, Section 1.4.2, with the exception of the following oligonucleotide primers used in this study. Forward primer: G24- AAT TCG AGC TCG CCC GGG GAT CCX GCT GGG CCC C, G30- AAT TCG AGC TCG CCC GGG GAT CCX GCT GGX CCC C , with X representing 8-oxoG. Reverse primer: 5Phos-ACT AAC CAG GCC CGA.

2.2.3 Substrate Preparation

The procedure was identical to that described in Chapter 1, Section 1.4.3.

2.2.4 Reconstitution

The procedure was identical to that described in Chapter 1, Section 1.4.4.

2.2.5 Characterization of reconstituted nucleosomes

The rotational positioning of the reconstituted nucleosomes was determined by DNaseI digestion. Free and nucleosomal substrates (7 μg DNA) were treated with 4 units of DNaseI (NEB) in 20 mM Tris-HCl (pH 7.6), 2.5 mM $MgCl_2$, 0.5 mM $CaCl_2$,100 mM NaCl at room temperature. Aliquots were removed after 0.5, 1, 2, 3, 5, and 10 minutes, and the reactions were stopped by the addition of 25 mM EDTA and heating at 90^{o} C for 5 min. The samples were phenol:chloroform extracted and loaded on a 12 % denaturing (7 M urea) polyacrylamide gel, 0.4 mm thickness, 21 cm × 50 cm. The gel was pre-warmed to 50 ^{o}C and lyophilized samples were loaded with a 80% formamide loading buffer containing 0.05% xylene cyanol and bromophenol blue, 1 mM EDTA and 10 mM

NaOH. Electrophoresis was carried out at 2300 V and 24 mA with 2X TBE as the running buffer. Visualization of the DNA cleavage products was carried out by autoradiography with a phosphoimager and FujiFilm Image Gauge software. One Maxam-Gilbert G-A lane was run on each gel in order to identify nucleotide bands.

2.2.6 Base Excision Repair Assays

Free and nucleosomal substrates (4 μg) were treated with BER enzymes hOGG1 (3.2 U) or Fpg (16 U) at similar molar concentrations at 37 ^{o}C. Reactions included APE1 (20 U), 10 mM Tris-HCL (pH 7.5), 10 mM $MgCl_2$, 100 mM NaCl, and 280 ng BSA. APE1 was utilized in the cleavage assays to increase the activity of the glycosylases by limiting their lyase activity. Aliquots were removed after 0, 1, 3, 5, 10, 15, and 30 minutes; the reactions were stopped by the addition of 25 mM EDTA and heating at 90^{o} C for 5 min. The samples were phenol:chloroform extracted and samples were loaded on a prepoured 15% TBE-urea gel (Invitrogen) with 80% formamide loading buffer containing 0.05% xylene cyanol and bromophenol blue, 1 mM EDTA and 10 mM NaOH. Visualization and densitometry of the assay products was carried out by autoradiography with a phosphoimager and FujiFilm Image Gauge software. Control samples were prepared as above in order to verify the stability of the nucleosomes during the course of the BER assays. Nucleosome samples were treated by the BER assays as described above with the exception of the phenol: chloroform extraction step. Samples were removed at 0, 5, 15, and 30 minutes, and the reactions were placed on ice. The nucleosomal samples were loaded on a 6% native PAGE (30.19:1, acrylamide/bisacrylamide) gel containing 5 % glycerol and run in 0.5X TBE at 220V. Autoradiography was utilized to visualize nucleosomal stability.

2.3 Results

2.3.1 Nucleosome Core Particle Formation and Rotational Analysis

Histones were extracted from chicken erythrocytes as previously described by Millard et al, 1998 and identified with SDS PAGE [26], figure 2.4. PCR was utilized to amplify the 154 bp fragment. The DNA substrates were subsequently 5'-^{32}P radiolabeled and wrapped with chicken histones using the reconstitution method as described by Millard et al [26]. Formation of nucleosome core particles produced a distinct gel shift on a 6% native PAGE and densitometry indicated a consistent wrapping efficiency of 85-95%, figure 2.5. Rotational accessibility of the nucleosome core particle was assessed with a DNaseI footprinting technique in which solution accessible minor groove sites were preferentially cleaved where the DNA was facing away from the histone protein. The DNaseI results were in agreement with previous DNaseI cleavage analysis of nucleosome substrates showing reduced cleavage in nucleosomal substrates with a 10 bp periodicity cleavage pattern indicative of alternating minor groove cleavage and correct nucleosomal rotational positioning [1,7,15 ,64-65]. Based on accessibility to DNaseI cleavage, two guanine sites in the 154 bp fragment that exhibited a contrast in rotational accessibility were chosen to be modified with an 8-oxoG. These were positions G24 and G30, figure 2.6. As illustrated by the DNaseI gel, G24 positioning is solution accessible and facing away from the histone in the minor groove. G30, being 6 base pairs away, has a rotational position that is in the minor groove closely apposed to the histone protein.

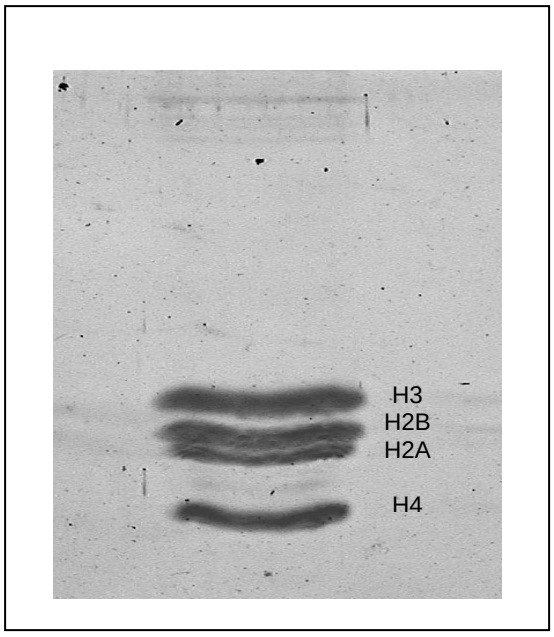

Figure 2.4 SDS PAGE gel showing histone sub-unit separation.

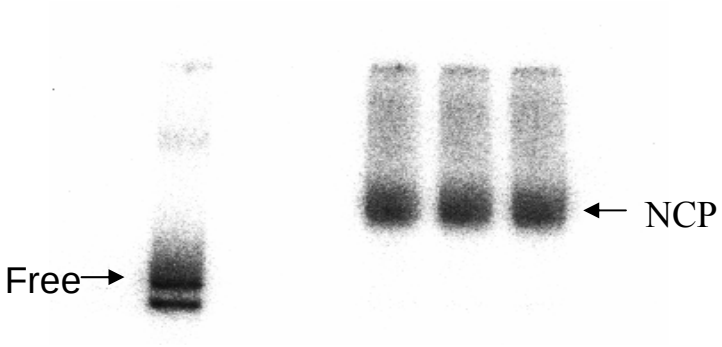

Figure 2.5 154 bp fragment of the *Xenopus borealis* 5S rRNA gene reconstituted into nucleosome core particles upon serial salt dilution in the presence of histone octamer, producing a characteristic gel shift in a native 5 % PAGE gel.

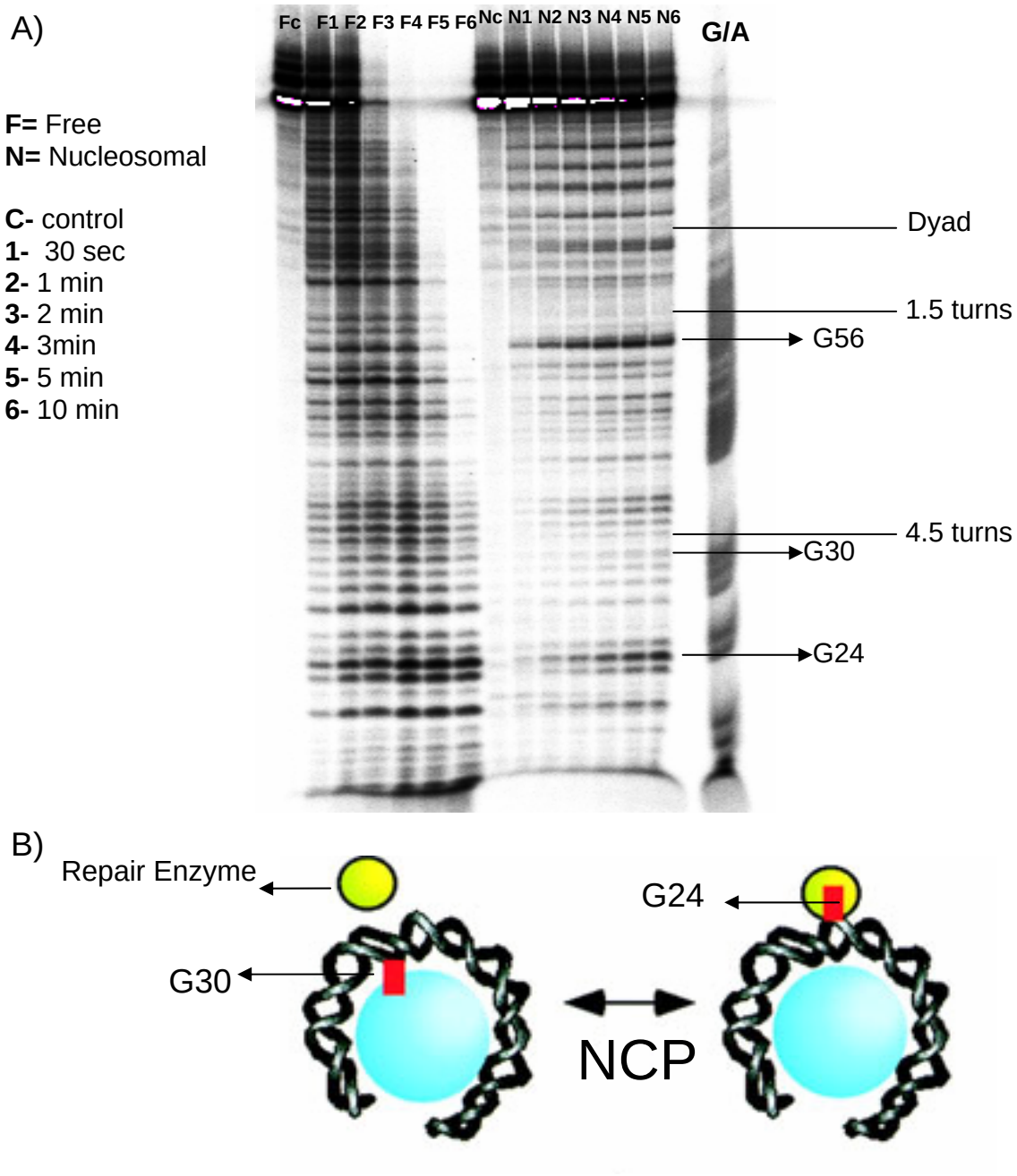

Figure 2.6 – A) Sequencing gel analysis of DNaseI footprinting of free and nucleosome core particles of the 154 bp fragment of the *Xenopus borealis* 5S RNA gene. Aliquots were removed after 0, 30 sec, 1, 2, 5, and 10 min, phenol:chloroform extracted and analyzed on a 12 % polyacrylamide urea sequencing gel. The "F" and "N" symbols represent, respectively, free and nucleosomal substrates. The lane marked G/A represent the Maxam-Gilbert chemical sequencing standard. B) NCP figure illustrating the rotational accessibility of G24 and G30. G24 and G30 positions are indicated by red squares.

Sequence of the *Eco*RI-*Rsa*I restriction fragment of the *Xenopus borealis* 5S rRNA gene

```
AATTCGAGCT CGCCCGGGGA TCCGGCTGGG CCCCCCCCAG AAGGCAGCAC
TTAAGCTCGA GCGGGCCCCT AGGCCGACCC GGGGGGGGTC TTCCGTCGTG

AAGGGGAGGA AAAGTCAGCC TTGTGCTCGC CTACGGCCAT ACCACCCTGA
TTCCCCTCCT TTTCAGTCGG AACACGAGCG GATGCCGGTA TGGTGGGACT

AAGTGCCCGA TATCGTCTGA TCTCGGAAGC CAAGCAGGGT CGGGCCTGGT
TTCACGGGCT ATAGCAGACT AGAGCCTTCG GTTCGTCCCA GCCCGGACCA

TAGT
ATCA
```

Figure 2.7-Sequence of the 154 bp wrapping fragment of the *Xenopus borealis* 5S rRNA gene. G24 and G30 are highlighted in red and PCR primers are underlined.

PCR was used to amplify the 154 bp fragment with the 8-oxoG lesion synthesized in the primer at positions G24 or G30, figure 2.7. The DNA substrates were subsequently 5'-^{32}P radiolabeled and wrapped around the chicken histones using the reconstitution method as described by Millard et al [26]. Formation of nucleosome core particles produced a distinct gel shift on a 6% native PAGE and densitometry indicated a consistent wrapping efficiency of 85-95%. Gel analysis indicated that reconstitution efficiency or stability were not influenced by placement of 8-oxoG in position G24 or G30 relative to unmodified wrapped DNA, figure 2.8.

The stability of the nucleosome core particles during BER glycosylase activity on 8-oxoG incorporated substrates (G24 and G30) was assessed with a 6% non-denaturing page gel. No disruption of the pre-formed nucleosome core particles was observed under the reaction buffering or temperature conditions required for BER activity for either hOGG1 or Fpg. Furthermore, the activity of Fpg and hOGG1 with the addition of APE1 did not disrupt core particle stability. This is indicated by the fact that the percentage of free DNA remained unchanged when pre-formed nucleosome core particles were subjected to Fpg and hOGG1 activity with APE1 at 37 ^{o} C, figure 2.8.

2.3.2 Nucleosomal BER Cleavage

The effect of the nucleosome core particle on the base excision of 8-oxoG by Fpg and hOGG1 was investigated by determining the cleavage activities of these enzymes on free and nucleosomal substrates. An 8-oxoG residue was placed at a defined position along the 154 bp wrapping fragment that correlated to an altered NCP solution accessibility (G24 and G30) as defined by DNaseI cleavage. Human apurinic/apyrimidinic endonuclease (APE1) was utilized to prevent the rate limiting step of lyase activity by the glycosylases and thereby increase glycosylase activity. The free and nucleosomal samples were treated under the same conditions and relative cleavages were compared by gel cleavage assays. The appearance of the smaller cleaved band is indicative of BER removal of the 8-oxoG lesion and subsequent APE1 DNA backbone cleavage. Densitometry using FujiFilm Image Gauge software was utilized to provide comparative enzyme activities with the percentage of lesion cleavage. Averages and standard deviations were taken from statistical analysis of 4 (Fpg) and 8 (hOGG1) experimental runs.

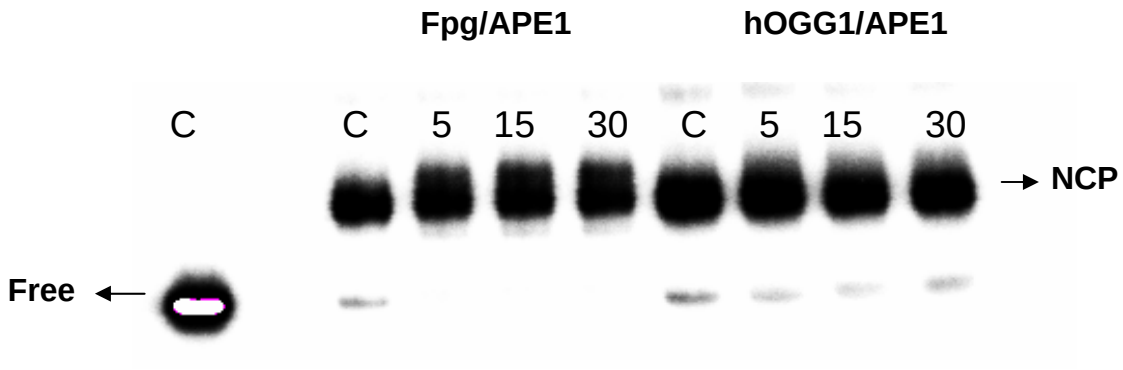

Figure 2.8- 154 bp fragment of the *Xenopus borealis* 5S rRNA gene with 8-oxoG incorporated into G24, reconstituted into nucleosome core particles upon serial salt dilution in the presence of histone octamer. NCP produced a characteristic gel shift in a native 5 % PAGE. Samples were subjected to 37 ^{o}C for 5, 15, and 30 min with BER enzymes Fpg and APE1 or hOGG1 and APE1. The "C" symbol represents controls in which APE1 was used but Fpg and hOGG1 were omitted.

The effect of the nucleosome on the activity of 8-oxoG removal by Fpg and hOGG1 was addressed by gel cleavage assays. Differences in enzyme cleavage efficiencies were seen in both free and nucleosomal substrates with approximate equimolar amounts of enzyme. Fpg provided increased cleavage of all samples relative to hOGG1 due to an increased molar activity which is described by increased units/mL by New England Biolabs (NEB); hOGG1 (1,600 units/mL), FPG (8,000 units/mL). Results indicated that both Fpg and hOGG1 activity have a sequence dependence on the position of 8-oxoG in naked DNA. A 1.4-2 fold increase in cleavage by hOGG1 and Fpg of the modified site G24 was observed relative to the G30 site in unwrapped samples. This data suggest that the BER glycosylase activity is influenced by the nucleobase chemistry surrounding the targeted lesion.

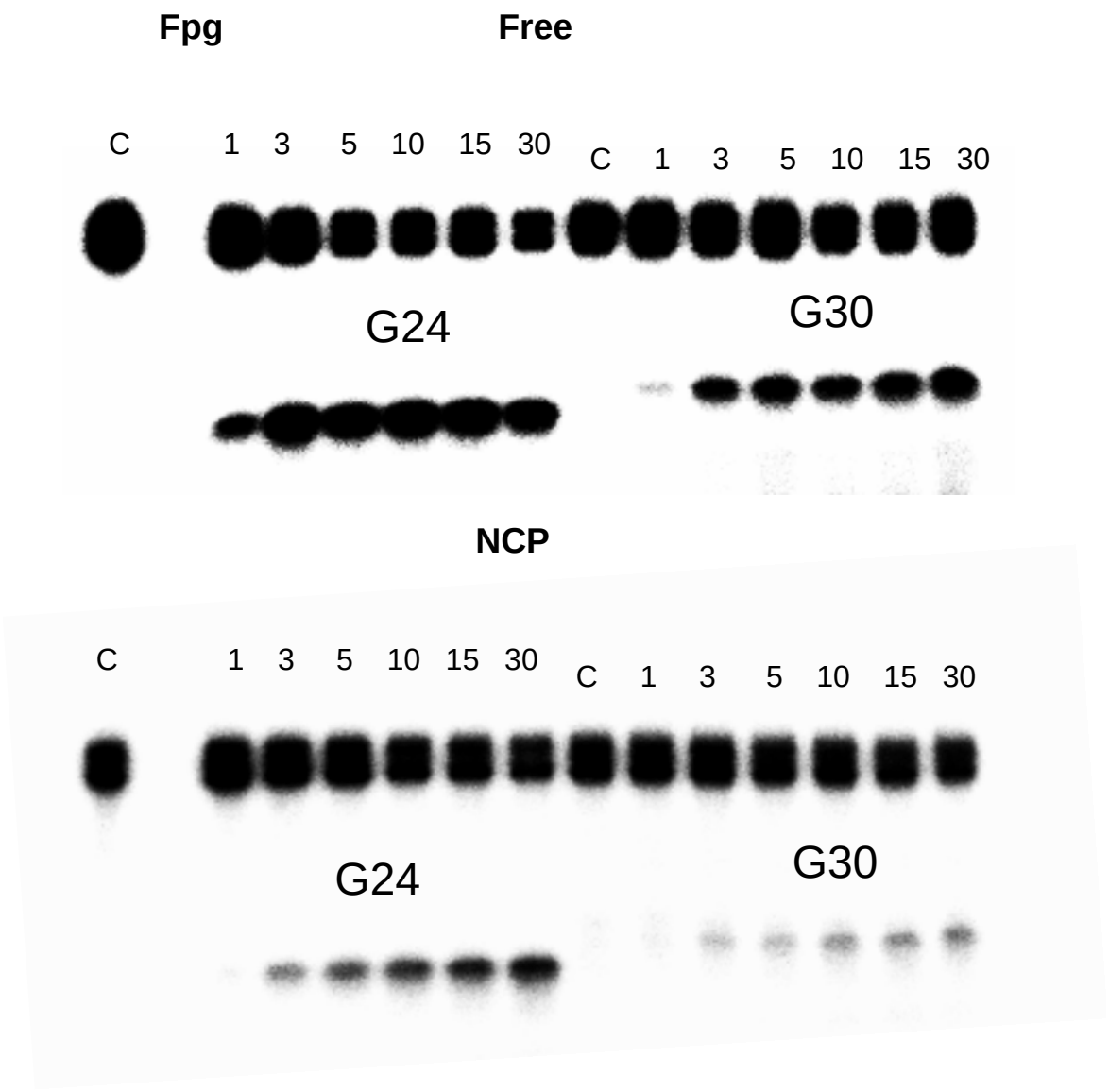

Figure 2.9 – Excision of 8-oxoG by the BER enzymes Fpg and APE1. A 15% urea gel showing the time course of excision of an internal 8-oxoG residue (G24 or G30) from naked DNA (Free) and nucleosomal core particles (NCP) at times 0, 1, 3, 5, 10, 15 and 30 min, with "C" being a control with no Fpg added.

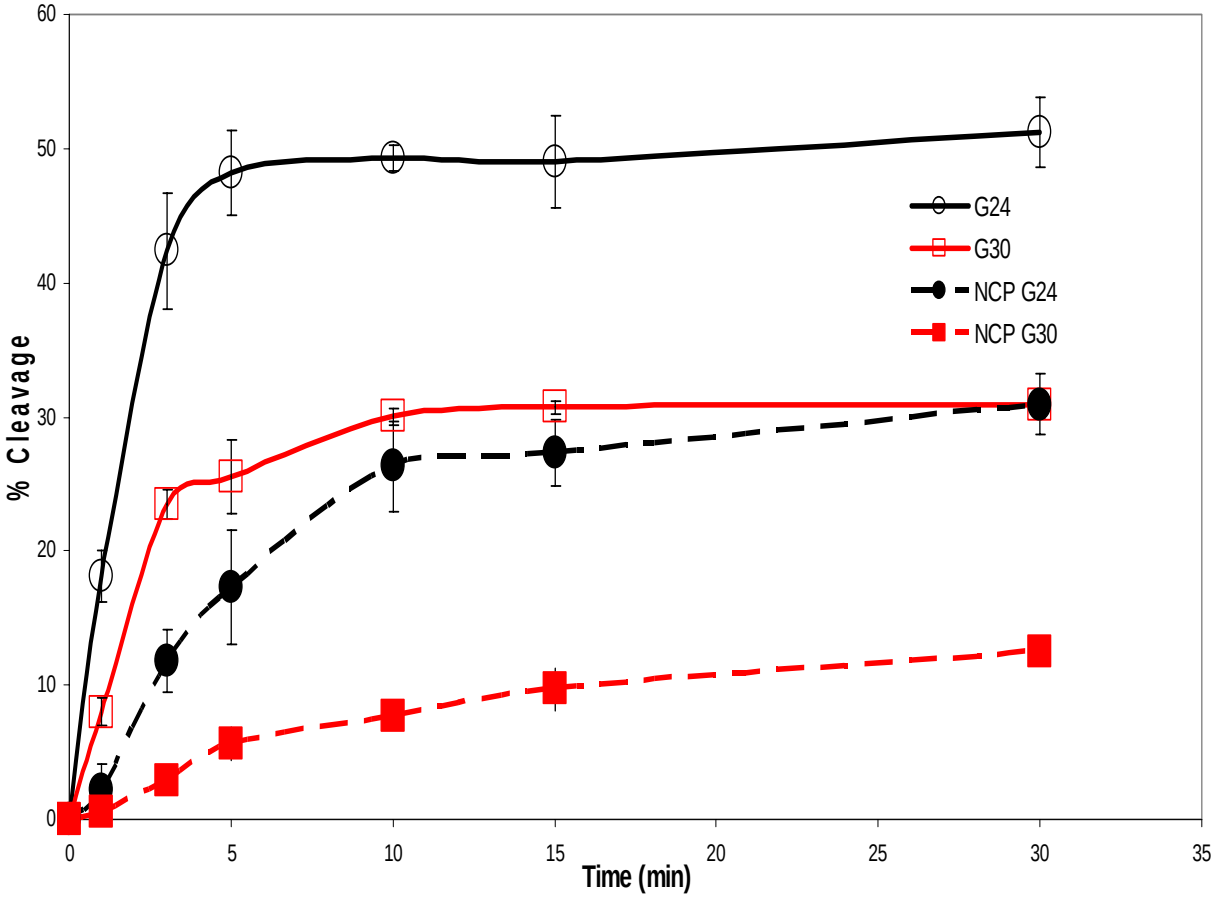

Figure 2.10 – Fpg and APE1 average rate of 8-oxoG excision from free (open) and NCP (closed) G24 and G30 substrates at 0, 1, 3, 5, 10, 15 and 30 min. Averages and standard deviations were taken from statistical analysis of 4 experimental runs.

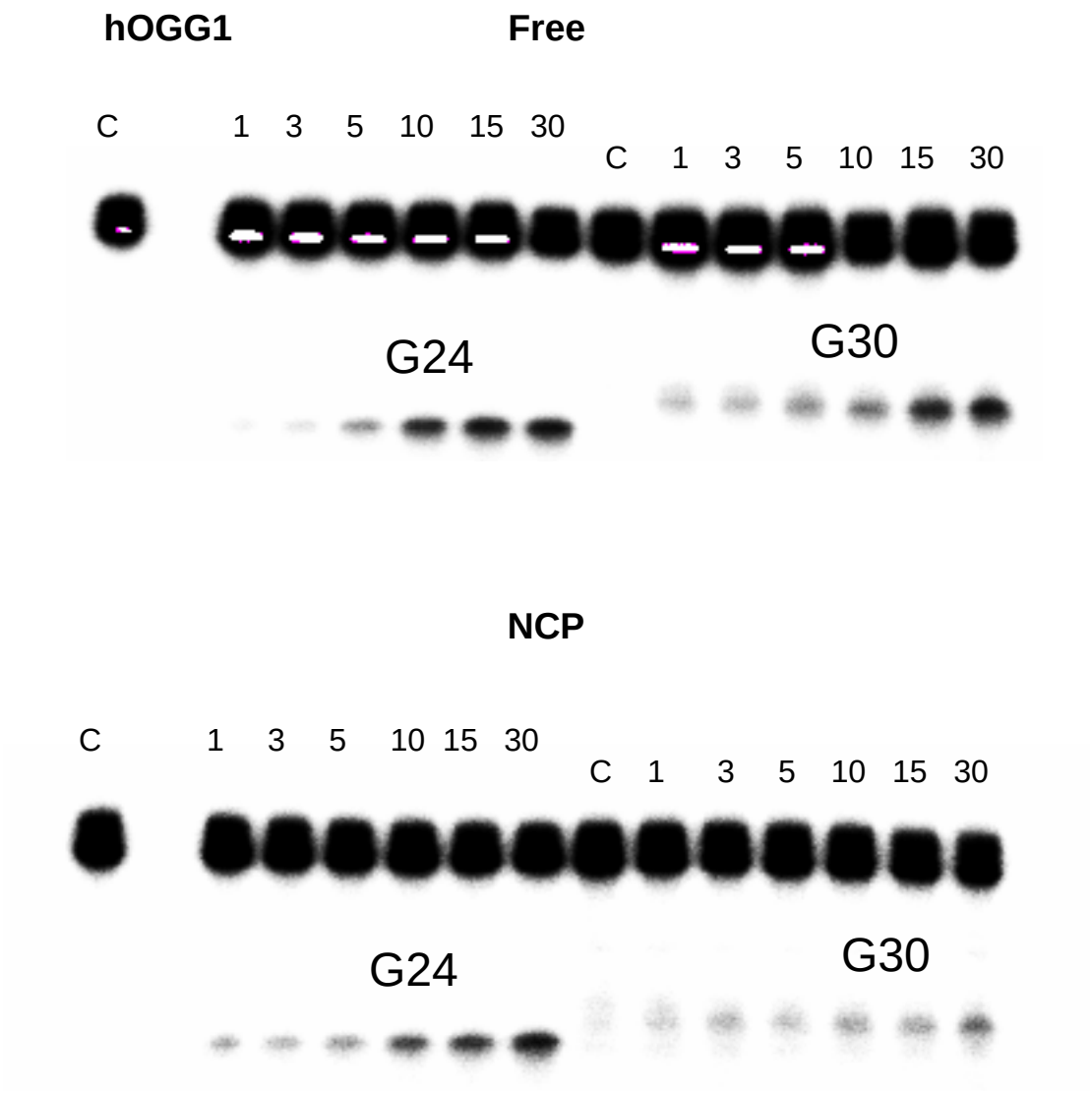

Figure 2.11 – Excision of 8-oxoG by the BER enzymes hOGG1 and APE1. A) 15% TBU gel showing the time course of excision of an internal 8-oxo G residue (G24 or G30) from naked DNA (Free) and nucleosomal core particle (NCP) at times 1, 3, 5, 10, 15 and 30 min, with "C" being a control with no hOGG1 added.

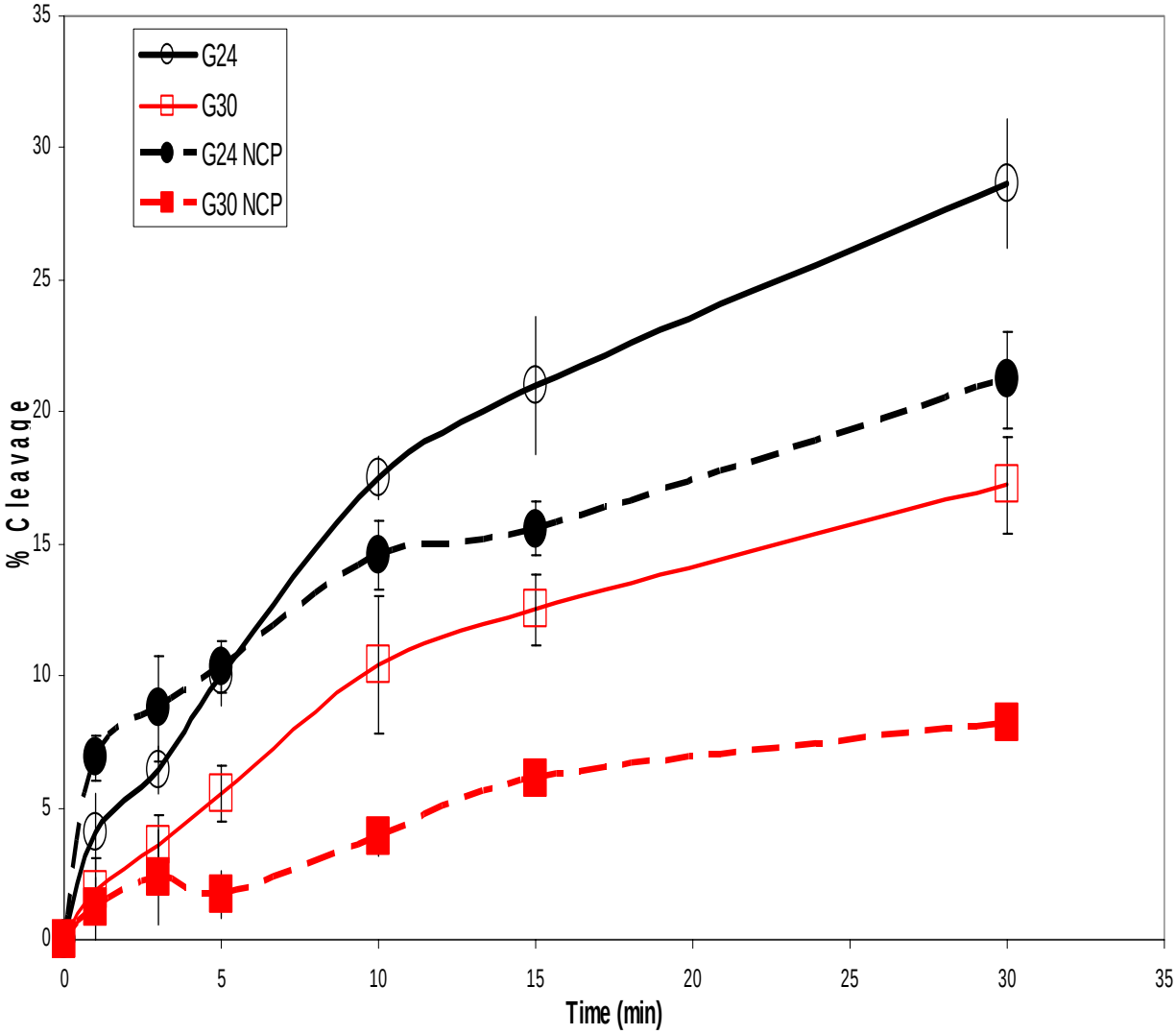

Figure 2.12 – hOGG1 and APE1 average rate of 8-oxoG excision from free (open) and NCP (closed) G24 and G30 substrates at 0, 1, 3, 5, 10, 15 and 30 min. Averages and standard deviations were taken from statistical analysis of 8 experimental runs.

The nucleosome decreased activity of both Fpg and hOGG1 by a maximum of 2.5 fold. Glycosylase cleavage of 8-oxoG also exhibited a rotational dependence towards the more solution accessible lesion as defined by DNase*I* footprinting. The G24 lesion exhibited enhanced cleavage relative to G30 in nucleosomal substrates for both glycosylases. Results also illustrated differences of relative cleavage efficiency of naked and wrapped substrates between the two glycosylases. hOGG1 exhibited smaller differences in cleavage efficiency of nucleosomal substrates relative to naked substrates than Fpg. Cleavage data graphed in figure 2.10 and 2.12 illustrated the apparent differences in Fpg and hOGG1 cleavage of free and nucleosomal substrates. The efficiency of Fpg reached a maximum after 10 min in contrast to hOGG1 which never reached a maximum even after 30 min. Relative differences of free and nucleosomal substrates were much smaller in hOGG1 samples versus Fpg. Early time points of hOGG1 indicated increased or equal cleavage efficiency of nucleosomal substrates relative to free DNA.

The ability of the nucleosome to alter BER cleavage efficiency by changing the solution accessibility through rotational positioning is seen by comparing the ratios of G24/G30 cleavage by Fpg and hOGG1. A similar sequence specificity for both enzymes was observed with free DNA substrates. Nucleosome formation dictated reduced cleavage to the G30 position by both Fpg and hOGG1, as indicated by the increased ratio of G24 to G30. The ratio of nucleosomal substrates also appeared to be very similar between the two enzymes indicating that neither enzyme was more efficient at dealing with a lesion that is facing the histone octamer, figure 2.13

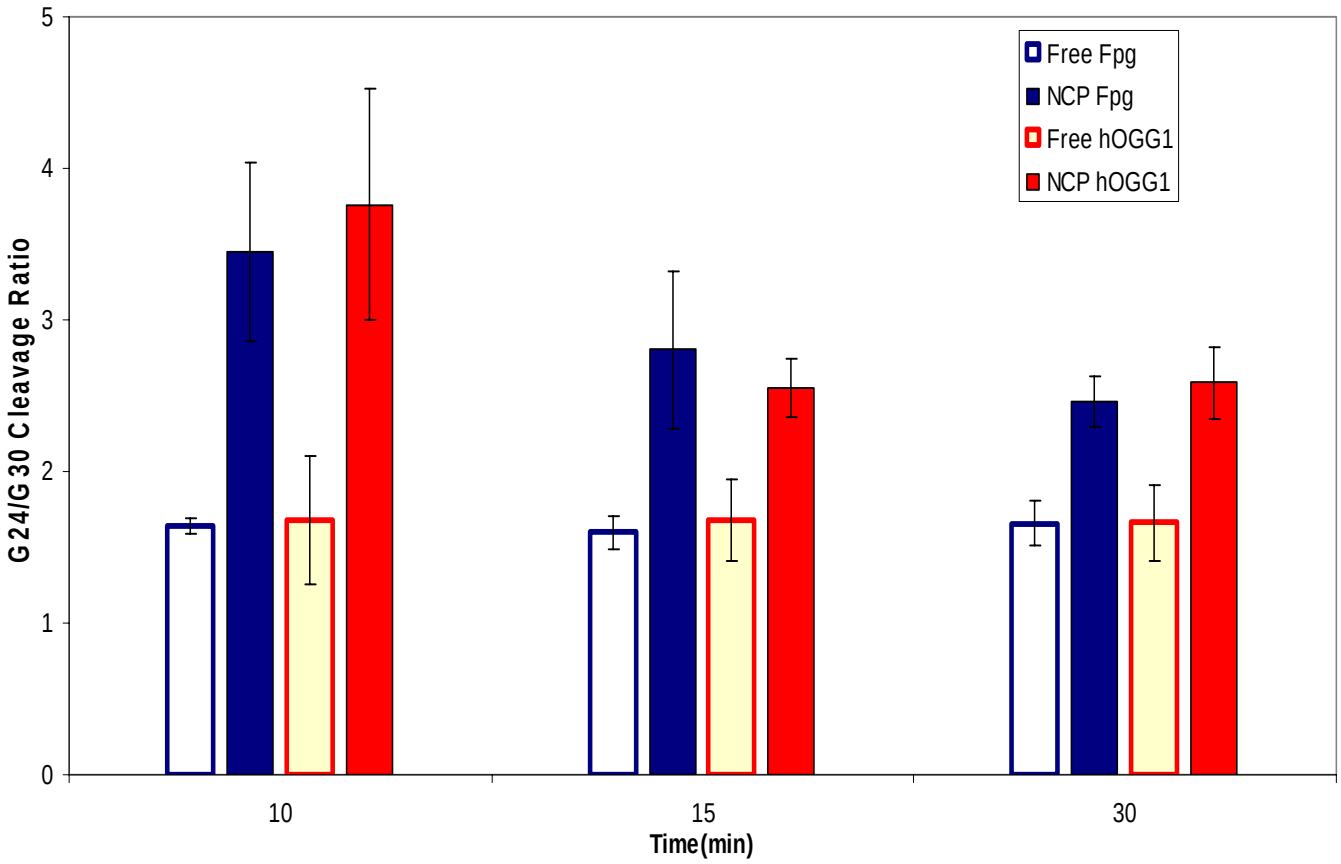

Figure 2.13- G24/G30 cleavage ratios of Free and Nucleosomal substrates by Fpg and hOGG1 at time points 10, 15 and 30 min. Averages and standard deviations were taken from statistical analysis of 4-8 experimental runs.

2.4 Discussion

This study addressed the question of how the BER glycosylase activity of hOGG1 and Fpg is affected by the nucleosomal environment. The prokaryote BER glycosylase Fpg does not function in the same nucleosomal environment *in vivo* as its eukaryotic counterpart hOGG1 but was used as a comparison. The activity of these two enzymes were investigated *in vitro* utilizing reconstituted nucleosome core particles. An 8-oxoG lesion was placed into two different positions on the 154 bp wrapping fragment that provided an altered rotational settings as demonstrated by DNaseI footprinting; G24 and G30. Lesion cleavage efficiency was measured for both modified DNA substrates in naked and nucleosomal DNA with both Fpg and hOGG1. It was determined that i) the position of the 8-oxoG lesion in naked DNA can significantly influence enzyme activity; ii) nucleosomal formation decreases the activity of these enzymes by a maximum of 2.5 fold and shows a rotational dependence with increased cleavage towards the more accessible lesion, G24; iii) the rotational dependence for both Fpg and hOGG1 were almost identical, however hOGG1 showed more efficient cleavage in the nucleosome setting relative to free DNA than Fpg did at shorter time points.

This study illustrated that both Fpg and hOGG1 activity is dependent on the positioning of 8-oxoG in naked DNA. A 1.4-2 fold increase in cleavage of G24 relative to G30 was observed for both hOGG1 and Fpg cleavage of naked DNA. While unexpected, Hirano et al., 2001 observed a similar result with up to a 10 fold difference in hOGG1 cleavage activity depending on the substrate sequence and 8-oxoG placement in naked DNA [66]. These data suggest that the BER glycosylase mechanism is influenced by the nucleobase chemistry surrounding the targeted lesion. It is known from

crystal structures that hOGG1 must flip out the targeted base into its active site, and plug the subsequent hole with the aryl ring of tyrosine to help sharply kink the DNA and improve access to the deoxyribose C1' [50]. It is likely that glycosylase activity is dependent on the ability (or resistance) of the lesion to be flipped out and kink the DNA. Since base sequence has long been known to impact DNA structural flexibility and thermodynamics, the local sequence surrounding the lesion could impact the efficiency of the BER glycosylase activity in this way. This thermodynamic dependence resembles the explanation utilized to explain the differences in repair rates by NER on different DNA adducts [33-36]. Differences could also be attributed to the kinetics of lesion recognition. Perhaps the surrounding sequence alters the lesion recognition kinetics of the BER glycosylases.

It should be noted that the cleavage efficiency of these BER enzymes correlates with the propensity of the oxidized guanine lesions to form based on their surrounding sequence. G24 is a 5' guanine of a guanine doublet, while G30 is the 3' guanine of a guanine triplet. Redox potential studies have illustrated that the 5'guanine in multiples is the most oxidation prone site, producing an oxidative hot spot. While it may be coincidental, it is interesting that a BER enzyme shows higher activity when the lesion is in a potential oxidative hot spot.

The nucleosome decreased the activity of these enzymes by a maximum of 2.5 fold and showed a rotational dependence with increased cleavage towards the more accessible lesion, G24. As illustrated by DNaseI cleavage, figure 2.6, naked DNA is more accessible than nucleosomal DNA. In addition, G24 is more accessible than G30 in the nucleosome due to rotational positioning. DNaseI binds and cleaves with higher

activity across the minor groove [65]. This infers that G24 is in the minor groove facing away from the histone and G30, half a turn away (6 bp), is in the minor groove facing the histone protein. Nucleosomal induced altered accessibility to these lesions explains Fpg and hOGG1's rotational dependence. BER enzymes can also be affected by nucleosome translational positioning, as seen by the impact of histone tails on enzyme FEN1 [57]. The rotational and translational positioning of G24 and G30 are illustrated in figure 2.14, and figure 2.15 respectively, using the crystal structure of the nucleosome core particle 1KX3 and Viewerlite software. Since the nucleosome in the crystal structure utilized a 146 bp wrapping fragment (palindromic DNA fragment derived from human α-satellite DNA) positioning similar to G24 and G30 was identified as cytosine21 and adenine27 in 1KX3 based on the rotational placement of G24 and G30 in this study. Cytosine21 and adenine27 were labeled 'G24' and 'G30' in figure 2.14, and figure 2.15. As depicted 'G24' is made more solution accessible than 'G30' through nucleosomal rotational placement, figure 2.14. Translational positioning of the nucleosome is such that 'G24' and 'G30' are over the H2A (yellow) and H2B (red) dimmer. The tail of H2B is in close proximity to both 'G24' and 'G30' suggesting that it could have interacted with the BER enzymes in this study, figure 2.15.

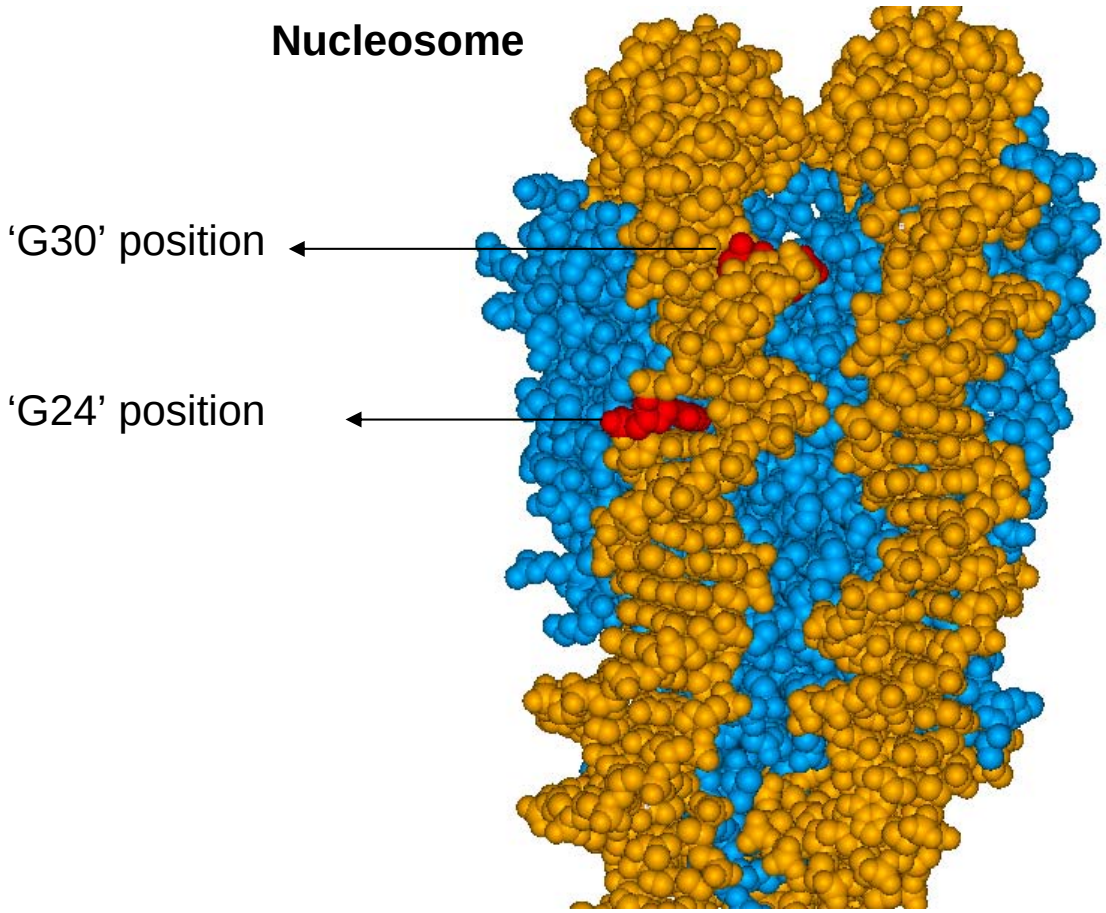

Figure 2.14- Crystal structure of the nucleosome illustrating rotational positioning of 'G24' and 'G30' lesions. The histone protein is represented in blue, DNA in orange and DNA bases matching the rotational positioning and placement of lesions G24 and G30 in this study are in red. Image was created using Viewerlite and PDB crystal 1KX3 [67].

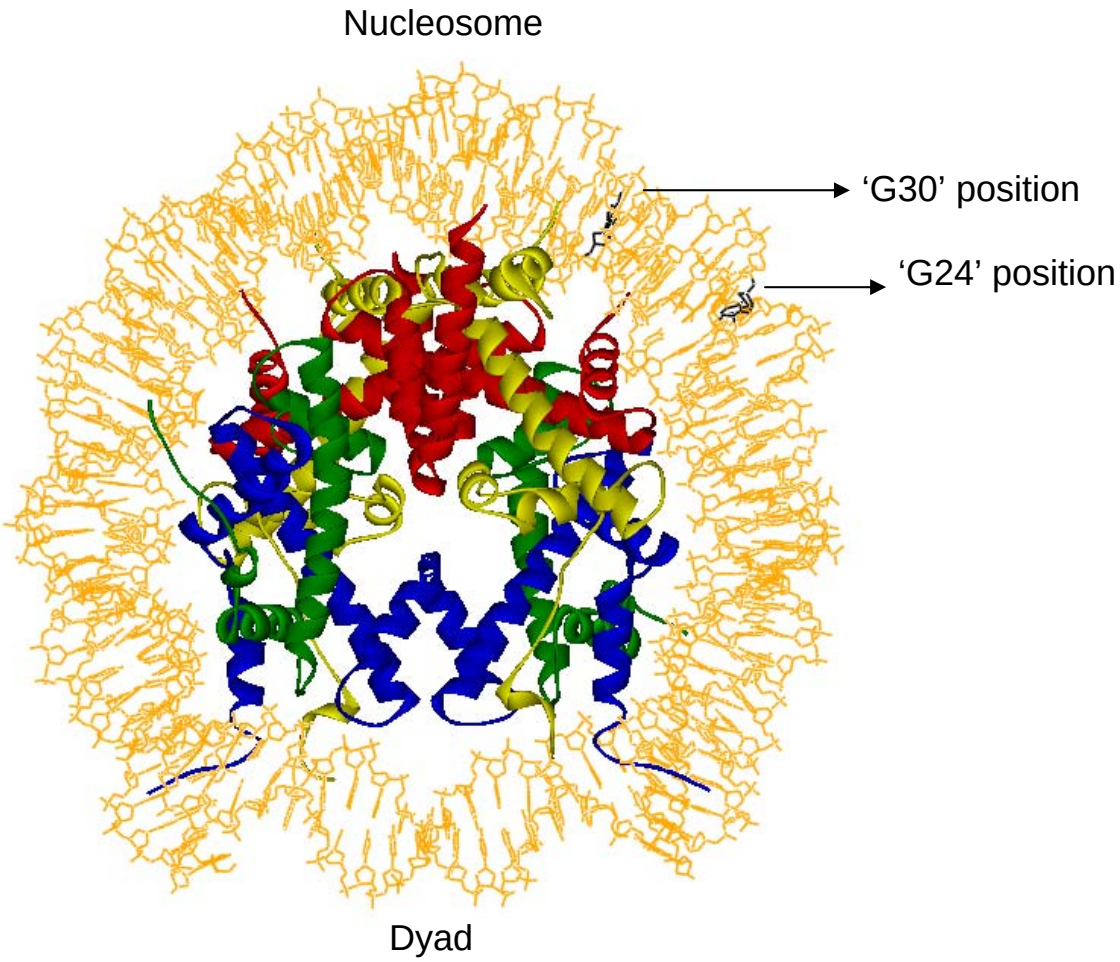

Figure 2.15- Crystal structure of the nucleosome illustrating translational positioning of 'G24' and 'G30' lesions. Histone is represented in standard histone sub-unit colors: yellow is H2A; red is H2B; Blue is H3; and Green is H4. DNA is orange and DNA bases matching the rotational positioning and placement of G24 and G30 lesions in this study are in black. Image was created using Viewerlite and PDB crystal 1KX3 [67].

hOGG1 and Fpg may also have an activity dependence on lesion recognition and cleavage in the major or minor groove independent of rotational placement in the nucleosome. It is well known that protein motifs present in eukaryotic transcription factors adopt highly ordered conformations specific to DNA rotation. The well characterized helix-turn-helix alpha helices motif found in homeodomain proteins and the zinc finger domain proteins bind primarily through contacts in the major groove [1]. Complementing such a mechanism with Fpg and hOGG1 is the fact that in duplex DNA the N7 guanine is more accessible in the major groove. Since it has been shown that the N7 of guanine is the main recognition site for Fpg and hOGG1 to distinguish between 8-oxoG, FapyG and Guanine [49-52] it seems possible that Fpg and hOGG1 would show a dependence towards major groove binding and lesion recognition. While there would be no dependence in naked DNA, solution accessibility in the nucleosome is rotationally limited and rotational placement (minor or major groove) of lesions facing away from the histone might further impact glycosylase efficiency through the kinetics of lesion recognition.

The rotational dependence for both Fpg and hOGG1 was almost identical, however hOGG1 showed slightly better cleavage in the nucleosomal setting relative to free DNA than Fpg. This infers that the increased activity of hOGG1 towards nucleosomal samples is not attributed to dealing with altered rotational accessibility, but perhaps is associated with the ability of hOGG1 to interact with the bulky electropositive histone octamer. As illustrated by figure 2.11 and 2.12 the activity of hOGG1 towards nucleosomal DNA at early time points is higher than that for naked DNA. This may be explained by interactions between hOGG1 and the histone octamer or a protein structure

that is less hindered by the histone protein than the Fpg. The fact that this trend doesn't continue at longer time points may be attributed to an increased binding that decreases the dissociation of the hOGG1-nucleosomal DNA complex. Increased binding would slow the kinetics of rebinding to other damaged nucleosomal substrates and subsequently decrease glycosylase activity. The process of binding and unbinding may be unnecessary *in-vivo* since nucleosome core particles are connected forming beads on a string. A processive enzyme that travels along the DNA may very well be the mechanistic route BER glycosylases utilize. In either case, this data suggests that the altered nucleosomal setting is inhibitory and presents a rotational dependence to BER. However, given the small relative differences of glycosylase excision in free and nucleosomal substrates, BER glycosylases may not require histone remodeling in order to carry out excision.

While the nucleosome provides a very different DNA setting the formation of the NCP doesn't appear to be very refractory towards BER glycosylase activity. The ratio of free/nucleosomal cleavage illustrates that these enzymes are active at a reduced activity of 1.4 to 2.5 fold. These values are comparative to the other studies in which BER activity was studied in the nucleosomal setting. Nilsen et al. reported a 3 to 9 fold reduction in uracil excision by the BER glycosylases UNG2 and SMUG1 with no rotational dependence [7]. Beard et al. 2003 also investigated uracil removal and repair with UDG and found the activity in the nucleosome to be reduced by a factor of ten with a rotational dependence of 2-3 fold [8]. The reduction of glycosylase cleavage seen in these studies is relatively small when compared to the efficiency of the independent repair processes of NER. Utilizing a NCP system Smerdon's group discovered that the individual activity of T4 endonucleaseV and *E. Coli* UV photolyase repair of a single UV

photoproduct (cis-syncylobutane thymine dimmer, CTD) on nucleosomal DNA was reduced 100-1000 fold relative to naked DNA [68]. However, when *Xenopus* oocyte nuclear extracts (contain all NER machinery) were utilized only a two fold reduction of DNA repair in the nucleosome was observed. This data provides further evidence for nucleosomal rearrangement during NER repair in addition to suggesting that BER glycosylase activity does not require nucleosomal rearrangement.

Studies (including this one) have shown slightly reduced rates of glycosylase activity in the nucleosome relative to naked DNA. These studies provide evidence for an independently working BER system that is not dependent on nucleosome rearrangement. The use of reconstituted nucleosomes has provided a controlled environment to better understand the workings of BER within the nucleosome. However, the *in vivo* environment is more variable with the formation of long continuous nucleosomal structures with altered levels of compactness and accessibility. Our understanding of the role of epigenetics, nucleosome rearrangements, and BER cooperativity is still premature and further experiments are needed to investigate the BER process in a more physiological setting.

2.5 References:

1. Wolfe, A. P., (2000) Chromatin: Structure and Function, 3rd Edition, Academic Press, NY.

2. Hayes, J., Wolffe, A. P., (1992) Transcription factor interaction with nucleosomal DNA. Bioessays.14, 597-603.

3. Anderson, J. D., Lowary, P. T., Widom, J. (2001) Effects of histone acetylation on the equilibrium accessibility of nucleosomal DNA target sites. J. Mol. Biol. 307, 977–985

4. Polach, K. J., Widom, J., (1995) Mechanism of protein access to specific DNA sequences in chromatin: a dynamic equilibrium model for gene regulation. J. Mol. Biol. 254, 130–149.

5. Polach, K. J., Widom, J., (1996) A model for the cooperative binding of eukaryotic regulatory proteins to nucleosomal target sites. J. Mol. Biol. 258, 800–812.

6. Hannon, R., Bateman, E., Allan, J., Harborne, N., Gould, H., (1984) Control of RNA polymerase binding to chromatin by variations in linker histone composition. J. Mol. Biol. 180, 131-49.

7. Nilsen, H., Lindahl, T., Verreault, A., (2002) DNA base excision repair of uracil residues in reconstituted nucleosome core particles. EMBO J. 21**,** 5943–5952.

8. Beard, B. C., Wilson, S. H., Smerdon, M. J., (2003) Suppressed catalytic activity of base excision repair enzymes on rotationally positioned uracil in nucleosomes. Proc. Natl. Acad. Sci. USA, 100, 7465–7470.

9. Beard, B. C., Stevenson, J. J., Wilson, S. H., Smerdon, M. J., (2005) Base excision repair in nucleosomes lacking histone tails. DNA Repair. 4**,** 203–209.

10. Smerdon, M. J., Conconi, A., (1999) Modulation of DNA damage and DNA repair in chromatin. Prog. Nucleic Acid Res. Mol. Biol. 62, 227–255.

11. Green, C. M., Almouzni, G., (2002) When repair meets chromatin. EMBO J. rep. 3, 28–33.

12. Hara. R., Mo, J., Sancar, A., (2000) DNA damage in the nucleosome core is refractory to repair by human excision nuclease. Mol. Cell. Biol. 20, 9173–9181.

13. Liu, X., Smerdon, M. J. (2000) Nucleotide excision repair of the 5S ribosomal RNA gene assembled into a nucleosome. J. Biol. Chem. 275, 23729–23735.

14. Kosmoski, J. V., Ackerman, E. J. and Smerdon, M. J., (2001) DNA repair of a single UV photoproduct in a designed nucleosome. Proc. Natl Acad. Sci. USA, 98, 10113–10118.

15. Noll, M., (1974) Internal structure of the chromatin subunit. Nature. London, 251, 249-251.

16. Noll, M., Kornberg, R.D., (1977) Action of micrococcal nuclease on chromatin and the location of histone H1. J. Mol. Biol.109, 393-404.

17. Ljungman, M., Hanawalt, P., (1992) Efficient protection against oxidative DNA damage in chromatin. Molecular Carcinogenesis. 5, 264-269.

18. Enright, H., Miller, W., Hebbel, R., (1992) Nucleosomal histone protein protects DNA from iron-mediated damage. Nucleic Acids Research. 20; 13, 3341-3346.

19. Chiu, S. M., Oleinick, N. L., (1982) Resistance of nucleosomal organization of eukaryotic chromatin to ionizing radiation. Radiat Res. 91; 3, 516-32.

20. Smith, B. L., Macleod, M. C., (1993) Covalent binding of the carcinogen benzo[a]pyrenediol epoxide to Xenopus laevis 5S DNA reconstituted into nucleosomes. J. Biol. Chem. 20, 620-629.

21. Thrall, B. D., Mann, D. B. Smerdon, M. J. Springer, D. L., (1994) Nucleosome structure modulates benzo[a]pyrenediol epoxide adduct formation. Biochemistry. 33, 2210-2216.

22. Smith, B. L., Bauer, G. B., Povirk., L. F., (1994) DNA damage induced by bleomycin, neocarzinostatin, and melphalan in a precisely positioned nucleosome-asymmetry in protection at the periphery of nucleosome-bound DNA. J. Biol. Chem. 269; 30, 587-30.

23. Galea A. M., Murray, V., (2002) The interaction of cisplatin and analogues with DNA in reconstituted chromatin. Biochimica et Biophysica Acta (BBA)/Gene Structure and Expression. 1579; 2, 142-152.

24. Pruss, D., Bushman, F. D., Wolfe, A.P., (1994) HIV integrase directs integration to sites of severe DNA distortion within the nucleosome core. Proc. Natl Acad. Sci. USA, 91, 5913-17.

25. Wong, J., Li, Q., Levi, B., Shi, Y., Wolffe, A. P., (1997) Structural and functional features of a specific nucleosome containing a recognition element for the thyroid hormone receptor. EMBO J. 16, 7130-7145.

26. Millard, J., Spencer, R., Hopkins, P., (1998) Effect of Nucleosome Structure on DNA Interstrand Cross-Linking Reactions. Biochemistry. 37, 5211-5219.

27. Liang, Q., Dedon, P., (2001) Cu(II)/H_2O_2- Induced DNA Damage is Enhanced by Packaging of DNA as a Nucleosome. Chem. Res. Toxicol. 4, 416-422.

28. Friedberg, E. C., Walker, G. C., Siede, W., (1995) DNA Repair and Mutagenesis. ASM Press, Washington, DC.

29. Friedberg, E. C., (2003) DNA damage and repair. Nature. 421**,** 436–440.

30. He, Z., Ingles, C. J., (1997) Isolation of human complexes proficient in nucleotide excision repair. Nucleic Acids Res. 25**,** 1136– 1141.

31. de Laat, W. L., Jaspers, N.G. J., Hoeijmakers, J. H. J., (1999) Molecular mechanism of nucleotide excision repair. Genes Dev. 13, 768–785.

32. Gillet, L., Scharer, O., (2006) Molecular Mechanisms of Mammalian Global Genome Nucleotide Excision Repair, Chem. Rev. 106, 253-276.

33. Gunz, D., Hess, M., Naegeli, H., (1996) Recognition of DNA Adducts by Human Nucleotide Excision Repair: Evidence for a thermodynamic probing mechanism. J. Biol. Chem. 271, 25089-25098.

34. Hess, M., Schwitter, U., Petretta, M., Giese, B., Naegeli, H., (1997) Bipartite substrate discrimination by human nucleotide excision repair. Proc. Natl. Acad. Sci. USA, 94, 6664.

35. Isaacs, R. J., Spielmann, H. P., (2004) A model for initial DNA lesion recognition by NER and MMR based on local conformational flexibility. DNA Repair. 3, 455–64.

36. Geacintov, N. E., Broyde, S., Buterin, T., Naegeli, H., Wu, M., Yan, S., Patel, D. J., (2002) Thermodynamic and structural factors in the removal of bulky DNA adducts by the nucleotide excision repair machinery. Biopolymers. 65, 202.

37. McCullough, A. K., Dodson, M. L., Lloyd R. S., (1999) Initiation of base excision repair: Glycosylase mechanisms and structures. Annu Rev Biochem. 68**,** 255–285.

38. Memisoglu, A., Samson, L., (2000) Base excision repair in yeast and mammals. Mutat Res. 451**,** 39–51.

39. Parikh S. S., Mol C. D., Slupphaug, G., Bharati, S., Krokan, H. E., Tainer, J. A., (1998) Base excision repair initiation revealed by crystal structures and binding kinetics of human uracil–DNA glycosylase with DNA. EMBO J. 17**,** 5214–5226.

40. Hosfield D. J., Daniels D. S., Mol C. D., Putnam C. D., Parikh S. S., Tainer J. A., (2001) DNA damage recognition and repair pathway coordination revealed by the structural biochemistry of DNA repair enzymes. Prog Nucleic Acid Res Mol Biol. 68**,** 315–347.

41. Jagannathan, I., Cole, H., Hayes, J., (2006) Base excision repair in nucleosome substrates, Chromosome Research. 14, 27-37

42. Ura, K., Hayes, J., (2002) Nucleotide excision repair and chromatin remodeling. Eur J Biochem. 269**,** 2288–2293.

43. Smerdon, M. J., Lieberman, M., (1978) Nucleosome rearrangement in human chromatin during UV-induced DNA- repair synthesis. Proc Natl Acad Sci. USA, 75 (9), 4238–4241.

44. Gontijo, A. M., Green, C. M., Almouzni, G., (2003) Repairing DNA damage in chromatin. Biochimie. 85**,** 1133–1147.

45. Smerdon, M.J., (1991) DNA repair and the role of chromatin structure. Curr. Opin. Cell Biol. 3, 422–428.

46. Wang, Z.G., Wu, X.H. and Friedberg, E.C., (1991) Nucleotide excision repair of DNA by human cell extracts is suppressed in reconstituted nucleosomes. J. Biol. Chem. 266, 22472–22478.

47. Sugasawa, K., Masutani, C., Hanaoka, F., (1993) Cell-free repair of UV-damaged simian virus 40 chromosomes in human cell extracts. I. Development of a cell-free system detecting excision repair of UV-irradiated SV40 chromosomes. J. Biol. Chem. 268, 9098–1004.

48. Araki, M., Masutani, C., Maekawa, T., Watanabe Y., Yamada, A., Sakai, D., Sugasawa, K., Ohkuma, Y., Hanaoka, F., (2000) Reconstitution of damage DNA excision reaction from SV40 minichromosomes with purified nucleotide excision repair proteins. Mutat. Res. 459, 147–160.

49. Slupphaug, G., Mol, C. D., Kavli, B., Arvai, A. S., Krokan, H. E., Tainer, J. A., (1996) A nucleotide-flipping mechanism from the structure of human uracil–DNA glycosylase bound to DNA. Nature. 384**,** 87–92.

50. Bruner, S., Norman, D., Verdine, G., (2000) Structural basis for recognition and repair of the endogenous mutagen 8-oxoguanine in DNA. Nature. 403, 859-866.

51. Banerjee, A., Verdine, G., (2006) A nucleobase lesion remodels the interaction of its normal neighbor in a DNA glycosylase complex. Proc. Natl. Acad. Sci. USA, 103, 15020-15025.

52. Fromme, C., Banerjee, A., Verdine, G., (2004) DNA glycosylase recognition and catalysis. Current Opinions in Structural Biology. 14, 43-49.

53. Radom, C. T., Banerjee, A., Verdine, G. L., (2007) Structural characterization of human 8-oxoguanine DNA glycosylase variants bearing active site mutations. J. Biol. Chem. 282, 9182-9194.

54. Hamm, M., Gill, T., Nicolson, S., Summers, M., (2007) Substrate specificity of Fpg (MutM) and hOGG1, two repair glycosylases. J. Am. Chem. Soc. 129 (25), 7724 -7725.

55. Chafin, D. R., Vitolo, J. M., Henricksen, L. A., Bambara, R. A., Hayes, J. J., (2000) Human DNA ligase I efficiently seals nicks in nucleosomes. The EMBO J. 19**,** 5492–5501.

56. Kysela, B., Chovanec, M., Jeggo, P. A., (2005) Phosphorylation of linker histones by DNA-dependent protein kinase is required for DNA ligaseIV-dependent ligation in the presence of histone H1. Proc. Natl Acad. Sci. USA. 102, 1877–1882.

57. Huggins, C. F., Chafin, D. R., Aoyagi, S., Henricksen, L. A., Bambara, R. A., Hayes, J. J., (2002) Flap endonuclease I efficiently cleaves base excision repair and DNA replication intermediates assembled into nucleosomes. Mol Cell. 10, 1201–1211.

58. Ames, B. N., Shigenaga, M. K., Hagen, T. M., (1993) Oxidants, antioxidants and the degenerative disease of aging. Proc. Natl. Acad. Sci. USA, 90, 7915-7922

59. Kasai, H., Nishimura, S., (1991) Oxidative Stress: Oxidants and Antioxidants (edited by Sies, H.) Academic Press. Ltd, London, 99-116.

60. Beckman, K. B., Ames, B. N., (1997) Oxidative decay of DNA, J. Biol. Chem. 272, 19633-19636.

61. Ames, B. N., Saul, R. L., (1987) Oxidative DNA damage, cancer and aging, Ann. Intern. Med. 107, 526-545.

62. Tchou, J., Kasai, H., Shibutani, S., Chung, M., Laval, J., Grollman, A. P., Nishimura, S., (1991) 8-oxoguanine DNA glycosylase and its substrate specificity. Proc. Natl. Acad. Sci. USA, 88, 4690-4694.

63. Vidal, A., Hickson, I., Boiteux, S., Radicella, P., (2001) Mechanism of stimulation of the DNA glycosylase activity of hOGG1 by the major human AP endonuclease: bypass of the AP lyase activity step. Nucleic Acids Research. 29 (6), 1285-1292.

64. Simpson, R. T., (1991) Nucleosome positioning: occurrence, mechanisms and functional consequences. Progr. Nucleic. Acids. Res. Mol. Biol. 40, 143-84.

65. Drew, H.R., (1984) Structural specificities of five commonly-used DNA nucleases. J. Mol. Biol. 176, 535-57.

66. Hirano, T., Hirano, H., Yamaguchi, R., Asami, S., Tsurudome, Y., Kasai, H., (2001) Sequence specificity of the 8-hydroxyguanine repair activity in rat organs. J. Radiat. Res. 42, 247-254.

67. Luger, K., Mader, A., Richmond, R., Sargent, D., Richmond, T., (1997) Crystal Structure of the Nucleosome Core Particle at 2.8 Å Resoltuion, Nature. 389, 251-260.

68. Kosmoski, J., Ackerman, E., Smerdon, M., (2001) DNA repair of a single UV photoproduct in a designed nucleosome. Proc. Natl Acad. Sci. USA, 98 (18), 10113-10118.

Chapter 3: DNA adduct 8-hydroxy-2'-deoxyguanosine inhibits *Not*I restriction enzyme activity

3.1 Introduction: DNA Oxidation, Methylation and Epigenetics

DNA methylation and histone modification play a crucial role in the epigenetic control of eukaryotic cells. Human tumor cells frequently have an altered expression of a number of genes due to altered cytosine methylation patterns [1-4]. However, both coding region mutations and altered methylation patterns can account for altered gene expression patterns and the loss of gene function [1, 5-7]. It has been reported throughout the literature that the number of cancer related genes affected by epigenetic inactivation equals or exceeds the number that are inactivated by mutation [4,6-10]. While many would argue for one route over another, it is very likely that both routes contribute to cancer formation and that the two process are intricately connected.

Epigenetic control through the methylation of cytosines is regulated by a family of proteins with a high affinity towards CpG dinucleotide sequences in DNA. These proteins known as methyl-binding proteins, MBP, have the ability to discriminate between oligonucleotides with methylated and unmethylated CpG dinucleotides [10-20]. After binding to CpG sequences MBP have been shown to recruit cytosine methyltransferase, histone deacetylases and other proteins involved in chromatin remodeling leading to the belief that the binding of MBP is an initial step in a complex epigenetic pathway involved in nucleosome condensation and gene silencing [10-27].

The hydrolytic deamination of methylated cytosine, 5-methylcytosine (5MeC), generates thymine residues producing not only an authentic mutation if replicated but also an inactive potential epigenetic site. While abnormal DNA methylation patterns

have been strongly correlated with cancer for over two decades, the influence of oxidative lesions on epigenetics is still poorly understood. 8-oxoG adduct formation has been attributed to genotoxicity and is a well known biomarker for oxidative DNA damage. Genotoxicity from this lesion is generally attributed to replication errors causing alterations in the primary DNA sequence that in turn can give rise to gene malfunction. However, a recent study illustrated that a single 8-oxoG adduct in a CpG site significantly inhibits the binding of a MBP, MeCP2 [28]. Complementing this result are studies showing that a single 8-oxoG adduct can significantly inhibit human and prokaryotic DNA methyltransferases as much as 13 fold [29,30]. These studies infer the ability of a single 8-oxoG adduct to regulate epigenetic changes usually ascribed to 5-methylcytosine. Thus, 8-oxoG has the ability to cause genetic alterations by altering epigenetics and or by inducing sequence mutations.

Restriction endonucleases are components of a restriction modification systems that utilize DNA methylation patterns and DNA degradation to protect bacteria from invading foreign DNA, such as bacteriophages [31]. Methylation patterns are used in this system to help distinguish between foreign and native DNA, and prevent native degradation by inhibiting the activity of many restriction endonucleases [32,33]. Type II restriction endonucleases cleave the phosphodiester bond at specific DNA sequences and lack methylase activity [31]. *Not*I is a type II DNA restriction endonuclease which exhibits inhibited enzyme activity upon CpG methylated sequences [32]. The purpose of this study is to examine the effect that an 8-oxoG lesion (placed in the recognition sequence) has on *Not*I cleavage compared with the inhibition seen upon DNA methylation.

3.2 Materials and Methods

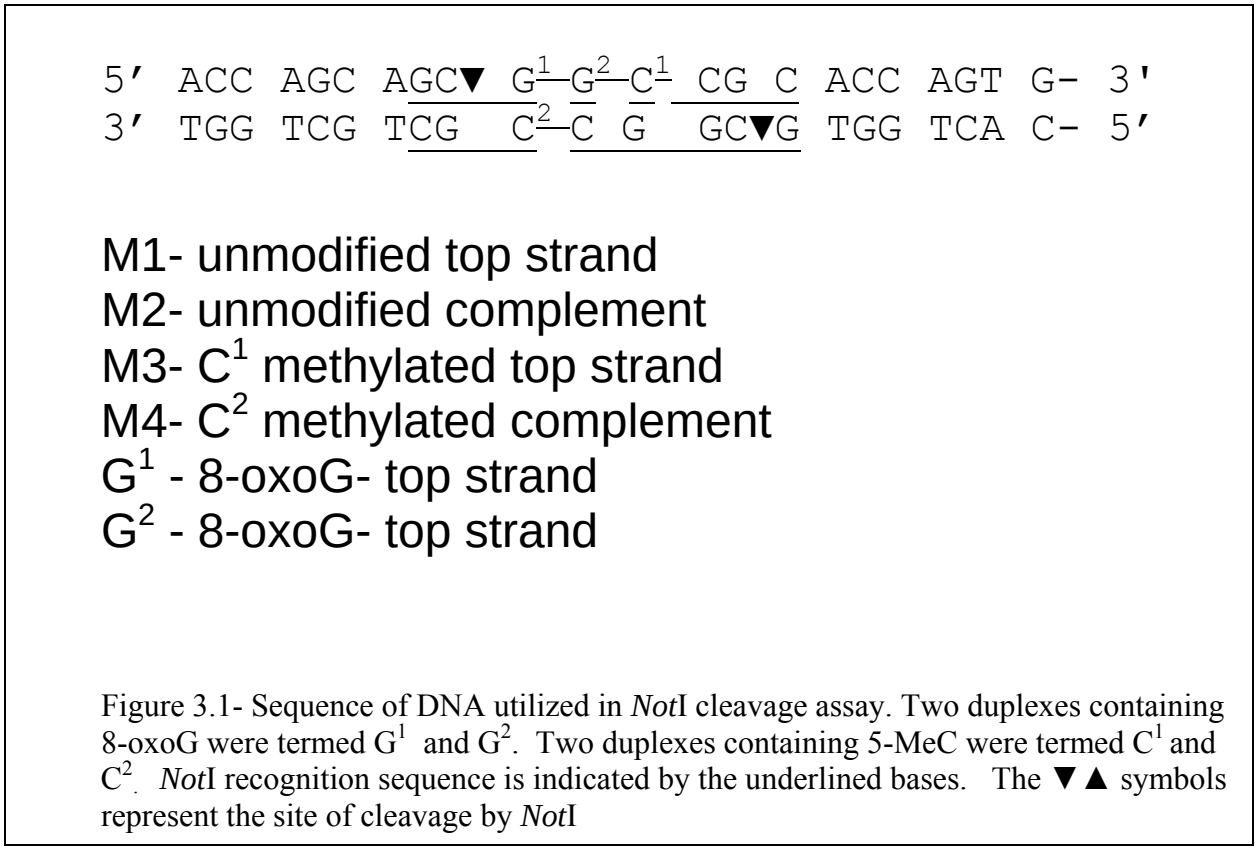

Figure 3.1- Sequence of DNA utilized in *Not*I cleavage assay. Two duplexes containing 8-oxoG were termed G^1 and G^2. Two duplexes containing 5-MeC were termed C^1 and C^2. *Not*I recognition sequence is indicated by the underlined bases. The ▼▲ symbols represent the site of cleavage by *Not*I

3.2.1 Substrate Preparation

Complimentary 24 mer oligonucleotides were purchased containing a central *Not*I restriction endonuclease recognition sequence. Modified oligonucleotides were purchased that incorporated 8-oxoG or 5-methylcytosine at two different positions in the *Not*I active site, G1, G2, or M1 and M2 respectively, figure 3.1. DNA oligonucleotides were quantified using A_{260} absorbance values. Single stranded 24 mer oligonucleotides were $5'^{32}P$ labeled by T4 polynucleotide kinase (New England Biolabs) with [γ-^{32}P] ATP (GM Healthcare) using 10 units of T4 polynucleotide kinase (T4 PNK, NEB) and 1x T4 PNK buffer at 37 ^{o}C for 40 min. Labeled oligonucleotides were purified with Micro Bio-Spin 6 (BioRad) columns. The labeled strand was incubated with 20% excess

of the unlabeled complementary strand utilizing a thermocycler. Oligos were heated to 90^{o} C for 5 min and then allowed to cool to room temperature slowly (1^{o} C per minute) to allow duplex formation. Five complexes were annealed; M2M1, M2G1, M2G2, M2M3, and M1M4.

3.2.2 Enzyme cleavage Efficiency

*Not*I restriction endonuclease was purchased from Promega (10 units/μl). Enzyme cleavage was assessed on DNA concentrations from 3 μM to 55 μM. Reaction volumes of 70 μl were utilized consisting of 1X Promega Buffer D, 1X Promega BSA, and 60 units of Promega *Not*I. Reactions were carried out at 37 ^{o} C. After the addition of *Not*I 10 μl aliquots of the reaction were removed at 15, 30, 45, 60, 75, and 90 min. Reactions were quenched with 10 μL of formamide loading buffer at 90 ^{o} C for 5 min. Cleavage efficiency was assessed with a 15% TBE Urea gel using autoradiography with Kodak BioMax MS Film.

3.3 Results

3.3.1 *Not*I cleavage assays

The oligo duplexes M2M1, M2G1, M2G2, M2M3, and M1M4 were labeled and annealed for the *Not*I cleavage assay. The assay was carried out on all five oligonucleotides with the same experimental conditions. Results were visualized with autoradiography with the appearance of a lower shifted band indicative of *Not*I activity. The unmodified oligo (M2M1) exhibited a strong cleavage pattern indicated by the intense gel shift, figure 3.2. The level of inhibition by the presence of 8-oxoG in the G1 or G2 position, or 5-methylcytosine in the C1 or C2 position is indicated by the cleavage product produced on the gels relative to M2M1. As illustrated, *Not*I cleavage assays

showed almost complete inhibition of activity by the presence of 8-oxoG at the G1 (M2G1) or G2 (M2G2) position. The extent of inhibition by 8-oxoG is similar to that seen with 5-methylcytosine in position C1 (M2M3) or C2 (M1M4), figure 3.2. Graphical representation of densitometry data from these gels depicts the similar intense level of inhibition by 5-methylcytosine and 8-oxoG, figure 3.3. Notice, the unmodified oligo (M1M2) reaches ~65 % cleavage while the modified oligos are all below 6 % cleavage.

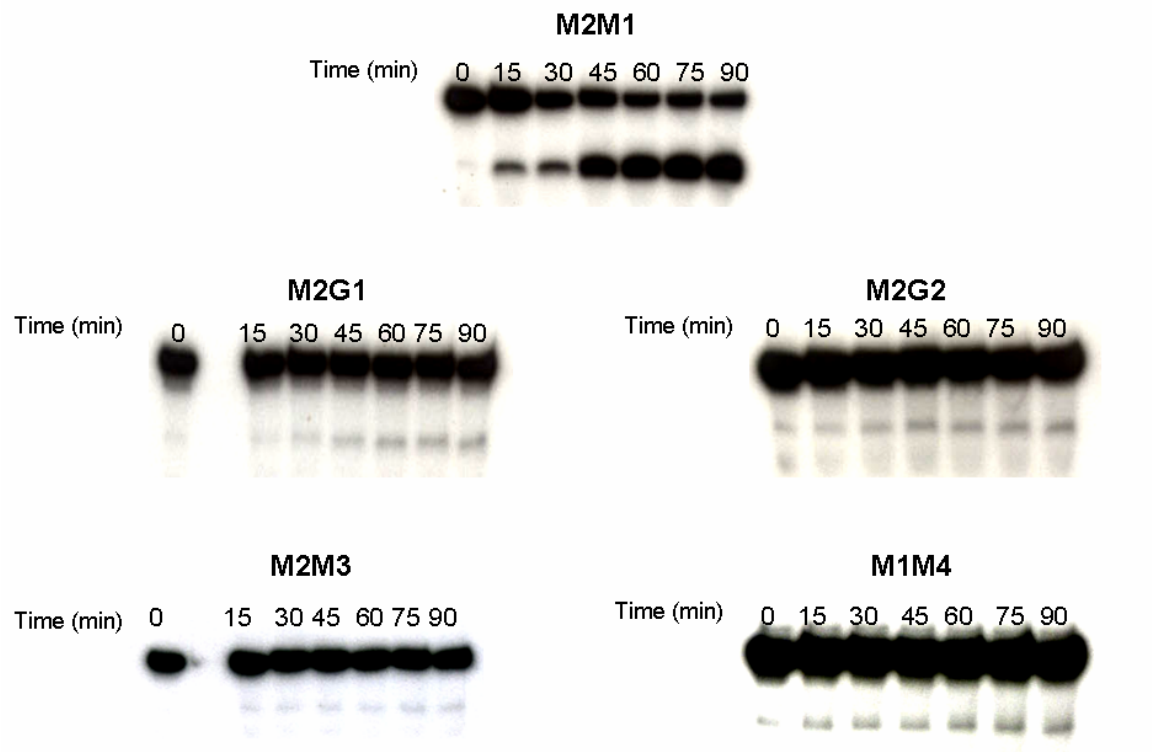

Figure 3.2- 15 % TBU denaturing gel of *NotI* cleavage assay of duplex 24 mers containing unmodified (M2M1) substrate and modified substrates. 8-oxoG at G1 (M2G1) and G2 (M2G2), 5-methylcytosine at C1 (M2M3) and C2 (M1M4). *Not*I activity was measured at 0, 15, 30, 45, 60, 75 and 90 min.

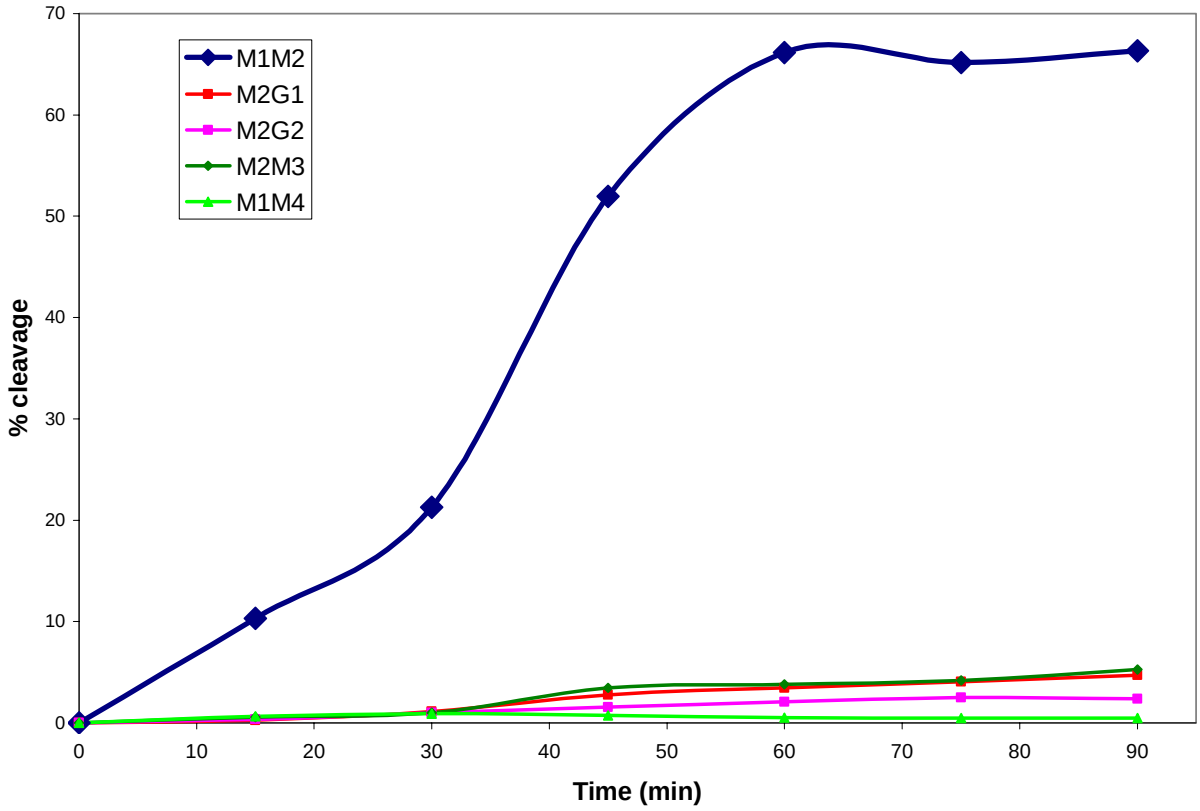

Figure 3.3- Graphical representation of *NotI* cleavage assay containing unmodified (M2M1) substrate and modified substrates. 8-oxoG at G1 (M2G1) and G2 (M2G2), 5-methylcytosine at C1 (M2M3) and C2 (M1M4). *Not*I activity was measured at 0, 15, 30, 45, 60, 75 and 90 min and graphed vs. percent cleavage.

3.4 Discussion

While very little is known about the potential mechanisms by which DNA damage can result in epigenetic changes, emerging studies indicate the role that oxidized lesions can play in altering epigenetics and their potential for causing cancer or disease states. Turk et al. investigated the efficiency of a human DNA methyltransferase to methylate a CpG dinucleotide containing an 8-oxoG lesion. This study illustrated that a single 8-oxoG lesion in the CpG site inhibited methylation of the adjacent cytosine

residue, but had limited effects on cytosine methylation when 8-oxoG was complemented to the target cytosine residue [29]. Valinluck et al, investigated the effect of oxidative damage to methyl CpG sequences on the binding of the methyl-CpG binding protein (MBP). The study observed that oxidative damage leading to 8-oxoG or 5-hydroxymethylcytosine formation in a CpG sequence significantly inhibited the binding of MBP [28]. Since MBP proteins are associated with epigenetic changes and gene down-regulation, oxidative events could play a large role in epigenetic regulation and gene dysfunction.

Complementary to the findings of previous studies we observed close to complete inhibition of the *Not*I restriction endonuclease when either an 8-oxoG or a 5-methylcytosine was placed into the recognition sequence of the enzyme. The level of inhibition was very significant, as illustrated by the large deviations in percent cleavage between the unmodified (M2M1) and modified oligonucleotides, figure 3.3. Furthermore, the inhibition by methylated oligos M2M3 and M1M4 matches the extent of *Not*I methylation inhibition by previous studies [32,33].

This study directly infers the possibility of an 8-oxoG lesion to affect the bacteria restriction modification system. Additionally, since DNA methylation in bacteria is involved in gene regulation, repair and control of cell cycle it is likely that 8-oxoG formation could affect these processes. While *Not*I is not involved in epigenetic programming this study illustrates the potential for DNA oxidative damage by the ubiquitous 8-oxoG lesion to completely inhibit enzymatic machinery in a similar manner to DNA methylation. Further studies are needed to investigate the impact of the 8-oxoG lesion on epigenetic processes in eukaryotic cell systems. In addition to 8-oxoG, further

oxidized guanine lesions (Sp and Gh) impact on epigenetic changes should also be evaluated. Given the fact that further oxidized lesions of guanine (Sp and Gh) are bulky and cause local DNA distortion it would be expected that their effects on epigenetics would be more detrimental than 8-oxoG lesions.

3.5 References

1. Herman, J. G., Baylin, S. B., (2003) Gene silencing in cancer in association with promoter hypermethylation. N Engl J Med. 349, 2042–54.

2. Feinberg, A. P., Tycko B., (2004) The history of cancer epigenetics. Nat Rev Cancer. 4, 143–153.

3. Esteller, M., (2005) Aberrant DNA methylation as a cancer-inducing mechanism. Annu Rev Pharmacol Toxicol. 45, 629–56.

4. Esteller, M., Silva, J. M., (2000) Dominguez G, et al., Promoter hypermethylation and BRCA1 inactivation in sporadic breast and ovarian tumors. J Natl Cancer Inst. 92, 564–9.

5. Jones, P., Laird, P., (1999) Cancer epigenetics comes of age. Nat Genet. 21, 163-7.

6. Jones, P., Baylin, S., (2002) The fundamental role of epigenetic events in cancer. Nat Rev Genet. 3, 415-28.

7. Herman, J. G., (1999) Hypermethylation of tumor suppressor genes in cancer. Biol. 9, 359-67.

8. Merlo, A., Herman, J., Moa, L., Lee, D. J., Gabrielson, E., Burger, P. C., Baylin, S. B., Sidransky, D., (1995) 5' CpG island methylation is associated with transcriptional silencing of the tumour suppressor p16/CDKN2/MST1 in human cancers. Nat Med. 1, 686-92.

9. Herman, J., Latif, F., Weng, Y., Lerman, M. I., Zbar, B., Liu, S., Samid, D., Duan, D. S., Gnarra, J. R., Linehan, et al., (1994) Silencing of the VHL tumor-suppressor gene by DNA methylation in renal carcinoma. Proc Natl Acad Sci. USA, 9, 19700-4.

10. Bird, A. P., Wolffe, A. P., (1999) Methylation-induced repression-belts, braces, and chromatin. Cell. 99, 451–454.

11. Nan, X., Meehan, R.R., Bird, A.P., (1993) Dissection of the methyl-CpG binding domain from the chromosomal protein MeCP2. Nucleic Acids Res. 21, 4886–4892.

12. Free, A., Wakefield , R. I., Smith, B. O., Dryden, D. T., Barlow, P. N., Bird, A. P., (2001) DNA recognition by the methyl-CpG binding domain of MeCP2. J. Biol. Chem. 276, 3353–3360.

13. Meehan, R. R., Lewis, J. D., Bird, A. P., (1992) Characterization of MeCP2, a vertebrate DNA binding protein with affinity for methylated DNA. Nucleic Acids Res. 20, 5085–5092.

14. Lewis, J. D., Meehan, R. R., Henzel, W. J., Maurer-Fogy, I., Jeppesen, P., Klein, F., Bird, A., (1992) Purification, sequence, and cellular localization of a novel chromosomal protein that binds to methylated DNA. Cell. 69, 905–914.

15. Magdinier, F., Wolffe, A. P., (2001) Selective association of the methyl-CpG binding protein MBD2 with the silent p14/p16 locus in human neoplasia. Proc. Natl Acad. Sci. USA, 98, 4990–4995.

16. Nguyen, C. T., Gonzales, F. A., Jones, P. A., (2001) Altered chromatin structure associated with methylation-induced gene silencing in cancer cells: correlation of accessibility, methylation, MeCP2 binding and acetylation. Nucleic Acids Res. 29, 4598–4606.

17. Nan, X., Bird, A., (2001) The biological functions of the methyl-CpG-binding protein MeCP2 and its implication in Rett syndrome. Brain Dev. 23, S32–S37.

18. Nan, X., Tate, P., Li, E., Bird, A., (1996) DNA methylation specifies chromosomal localization of MeCP2. Mol. Cell. Biol. 16, 414–421.

19. Holliday, R., Ho, T., (2002) DNA methylation and epigenetic inheritance. Methods. 27, 179–183.

20. Bhakat, K. K., Mitra, S., (2003) CpG methylation-dependent repression of the human O_6-methylguanine DNA methyltransferase gene linked to chromatin structure alteration. Carcinogenesis. 24, 1337–1345.

21. Kimura, H., Shiota, K., (2003) Methyl-CpG-binding protein, MeCP2, is a target molecule for maintenance DNA methyltransferase, Dnmt1. J. Biol. Chem. 278, 4806–4812.

22. Fuks, F., Hurd, P. J., Wolf, D., Nan, X., Bird, A. P., Kouzarides, T., (2003) The methyl-CpG-binding protein MeCP2 links DNA methylation to histone methylation. J. Biol. Chem. 278, 4035–4040.

23. Nan, X., Ng, H. H., Johnson, C. A., Laherty, C. D., Turner, B. M., Eisenmann, R. N., Bird, A., (1998) Transcriptional repression by the methyl-GpG-binding protein MeCP2 involved a histone deacetylase complex. Nature. 393, 386–389.

24. Knoepfler, P. S., Eisenman, R. N., (1999) Sin meets NuRD and other tails of repression. Cell. 99, 447–450.

25. Jones, P. L., Veenstra, G. J., Wade, P. A., Vermaak, D., Kass, S. U., Landsberger, N., Strouboulis, J., Wolffe, A. P., (1998) Methylated DNA and MeCP2 recruit histone deacetylase to repress transcription. Nature Genet. 19, 187–191.

26. Ng, H.-H., Zhang, Y., Hendrich, B., Johnson, C. A., Turner, B. M., Erdjument-Bromage, H., Tempst, P., Reinberg, D., Bird, A., (1999) MBD2 is a transcriptional repressor belonging to the MeCP1 histone deacetylase complex. Nature Genet. 23, 58–61.

27. Ng, H.-H., Jeppesen, P., Bird, A., (2000) Active repression of methylated genes by the chromosomal protein MBD1. Mol. Cell. Biol. 20**,** 1394–1406.

28. Valinluck, V., Tsai, H., Rogstad, D., Burdzy, A., Bird, A., Sowers, L., (2004) Oxidative damage to methyl-CpG sequences inhibits the binding of the methyl-CpG binding domain (MBD) of methyl-CpG binding protein 2 (MeCP2), Nucleic Acids Research. 32;14, 4100-4108.

29. Turk, P., Laayoun, A., Smith, S., Weitzman, S., (1995) DNA adduct 8-hydroxyl-2'-deoxyguanosine (8-hydroxyguanine) affects function of human DNA methyltransferase. Carcinogensis.16;5, 1253-1255.

30. Weitzman, S., Turk, P., Milkowski, D., Kozlowski, K., (1994) Free radical adducts induce alterations in DNA cytosine methylation. Proc. Natl Acad. Sci. USA, 91, 1261-1264.

31. Pingoud, A., Fuxreiter, M., Pingoud, V., Wende, W., (2005) Type II restriction endonucleases: structure and function. Cellular and Molecular Life Sciences. 62, 685-707.

32. McClelland, M., Nelson, M., (1985) The effect of site specific methylation on restriction endonuclease digestion. Nucleic Acids Research. 13, 201-207.

33. McClelland, M., (1981) The effect of sequence specific DNA methylation on restriction endonuclease cleavage. Nucleic Acids Research. 9, 5859-5866.